

AMINO ACID POSITION-SPECIFIC CONTRIBUTIONS TO AMYLOID β - PROTEIN OLIGOMERIZATION[†]

Samir K. Maji^{1,6}, Rachel R. Ogorzalek Loo^{2,3}, Mohammed Inayathullah¹, Sean M. Spring¹,
Sabrina S. Vollers^{1,7}, Margaret M. Condrón¹, Gal Bitan^{1,3,4}, Joseph A. Loo^{2,3,5}, and David
B. Teplow^{1,3,4*}

From ¹Department of Neurology and ²Department of Biological Chemistry, David Geffen School of
Medicine; ³Molecular Biology Institute; ⁴Brain Research Institute; and ⁵Department of Chemistry and
Biochemistry, University of California, Los Angeles, California 90095

Running title: Control of A β oligomerization

⁶Current address: School of Bioscience and Bioengineering, IIT Bombay, Powai, Mumbai 400076, India

⁷Current address: Department of Biochemistry and Molecular Pharmacology, University of Massachusetts
Medical School, Worcester, MA 01655

*Address correspondence to: David B. Teplow, Ph.D., 635 Charles E. Young Drive South (Room 445),
Los Angeles, CA 90095-7334; E-Mail: dteplow@ucla.edu

Understanding the structural and assembly dynamics of the amyloid β -protein (A β) has direct relevance to the development of therapeutic agents for Alzheimer's disease. To elucidate these dynamics, we combined scanning amino acid substitution with a method for quantitative determination of the A β oligomer frequency distribution, Photo-Induced Cross-linking of Unmodified Proteins (PICUP), to perform "scanning PICUP." Tyr, a reactive group in PICUP, was substituted at position 1, 10, 20, 30, or 40 (for A β 40) or 42 (for A β 42). The effects of these substitutions were probed using circular dichroism spectroscopy, Thioflavin T binding, electron microscopy, PICUP, and mass spectrometry. All peptides displayed a RC \rightarrow α / β \rightarrow β transition, but substitution-dependent alterations in assembly kinetics and conformer complexity were observed. Tyr¹-substituted homologues of A β 40 and A β 42 assembled slowest and yielded unusual patterns of oligomer bands in gel electrophoresis experiments, suggesting oligomer compaction had occurred. Consistent with this suggestion was the observation of relatively narrow [Tyr¹]A β 40 fibrils. Substitution of A β 40 at the C-

terminus decreased the population conformational complexity and substantially extended the highest order of oligomers observed. This latter effect was observed in both A β 40 and A β 42 as the Tyr substitution position number increased. The ability of a single substitution (Tyr¹) to alter A β assembly kinetics and the oligomer frequency distribution suggests that the N-terminus is not a benign peptide segment, but rather that A β conformational dynamics and assembly are affected significantly by the competition between the N- and C-termini to form a stable complex with the central hydrophobic cluster.

Alzheimer's disease (AD) is the most common cause of late-life dementia (1) and is estimated to afflict more than 27 million people worldwide (2). An important etiologic hypothesis is that amyloid β -protein (A β) oligomers are the proximate neurotoxins in AD. Substantial *in vivo* and *in vitro* evidence supports this hypothesis (3-12). Neurotoxicity studies have shown that A β assemblies are potent neurotoxins (5, 13-20) and the toxicity of some oligomers can be greater than that of the corresponding fibrils (21). Soluble A β oligomers

inhibit hippocampal long term potentiation (LTP) (4, 5, 13, 15, 17, 18, 22) and disrupt cognitive function (23). Compounds that bind and disrupt the formation of oligomers have been shown to block the neurotoxicity of A β (24, 25). Importantly, recent studies in higher vertebrates (dogs) have shown that substantial reduction in amyloid deposits in the absence of decreases in oligomer concentration has little effect on recovery of neurological function (26).

Recent studies of A β oligomers have sought to correlate oligomer size and biological activity. Oligomers in the supernates of fibril preparations centrifuged at $100,000 \times g$ caused sustained calcium influx in rat hippocampal neurons, leading to calpain activation and dynamin 1 degradation (27). A β -derived diffusible ligand (ADDL)-like A β 42 oligomers induced inflammatory responses in cultured rat astrocytes (28). A 90 kDa A β 42 oligomer (29) has been shown to activate ERK1/2 in rat hippocampal slices (30) and bind avidly to human cortical neurons (31), in both cases causing apoptotic cell death. A comparison of the time-dependence of the toxic effects of the 90 kDa assembly with that of ADDLs revealed a five-fold difference, ADDLs requiring more time for equivalent effects (31). A 56 kDa oligomer, "A β *56," was reported to cause memory impairment in middle-aged transgenic mice expressing human APP (32). A nonamer also had adverse effects. Impaired LTP in rat brain slices has been attributed to A β trimers identified in media from cultured cells expressing human APP (33). Dimers and trimers from this medium also have been found to cause progressive loss of synapses in organotypic rat hippocampal slices (10). In mice deficient in neprilysin, an enzyme that has been shown to degrade A β in vivo (34), impairment in neuronal plasticity and cognitive function correlated with significant increases in A β dimer levels and synapse-associated A β oligomers (35).

The potent pathologic effects of A β oligomers provide a compelling reason for elucidating the mechanism(s) of their formation. This has been a difficult task because of the metastability and polydispersity of A β assemblies (36). To obviate these problems, we introduced the use of the method of Photo-Induced Cross-linking of Unmodified Proteins

(PICUP) to rapidly (<1 sec) and covalently stabilize oligomer mixtures (for reviews, see (37, 38)). Oligomers thus stabilized no longer exist in equilibrium with monomers or each other, allowing determination of oligomer frequency distributions by simple techniques such as SDS-PAGE (37). Recently, to obtain population-average information on contributions to fibril formation of amino acid residues at specific sites in A β , we employed a scanning intrinsic fluorescence approach (39). Tyr was used because it is a relatively small fluorophore, exists natively in A β , and possesses the side-chain most reactive in the PICUP chemistry (40). Using this approach, we found that the central hydrophobic cluster region (Leu17–Ala21) was particularly important in controlling fibril formation of A β 40 whereas the C-terminus was the predominant structural element controlling A β 42 assembly (39). Here, we present results of studies in which key strategic features of the two methods have been combined to enable execution of "scanning PICUP" and the consequent revelation of site-specific effects on A β oligomerization.

EXPERIMENTAL PROCEDURES

Chemicals and reagents. Chemicals were obtained from Sigma and were of the highest purity available. Water was double-distilled and deionized using a Milli-Q system (Millipore Corp., Bedford, MA).

Peptide design and synthesis. In addition to studying native A β 40 and A β 42, each of which contains Tyr10, single Tyr substitutions were made in each A β alloform at Asp1, Phe20, Ala30, and the C-terminus (Val40 or Ala42) (Fig. 1). In each non-native peptide, Tyr10 was replaced by Phe, which is largely unreactive in PICUP, so that data interpretation would not be complicated by multiple potential cross-linking sites. A similar substitution strategy proved effective in Tyr intrinsic fluorescence studies (39) in which Phe was fluorometrically, as opposed to chemically, insignificant. A β synthesis, purification, and characterization were done as described (41). Briefly, A β 40, A β 42, and their Tyr-substituted peptides (Fig. 1) were made on an automated peptide synthesizer

(Model 433A, Applied Biosystems, Foster City, CA) using 9-fluorenylmethoxycarbonyl-based methods. Peptides were purified using reversed-phase high-performance liquid chromatography (RP-HPLC). Quantitative amino acid analysis and mass spectrometry yielded the expected compositions and molecular weights, respectively, for each peptide. Purified peptides were stored as lyophilizates at -20°C . When possible, in order to maximize chemical homogeneity among related peptides, multiple peptides were synthesized from the same starting resin by resin splitting at sites of sequence variation. A β 40 and its Tyr-substituted analogues were synthesized using preloaded [Val]Wang resin. A β 42 and its Tyr-substituted analogues were made in analogous manner using preloaded [Ala]Wang resin. Peptides [Tyr⁴⁰]A β 40 and [Tyr⁴²]A β 42 were synthesized using preloaded [Tyr]Wang resin.

Sample preparation. All peptides were pretreated with dilute NaOH to increase their solubility and decrease *de novo* peptide aggregation (42). Briefly, peptides were dissolved initially in 2 mM NaOH (1 mg/ml), sonicated for 3 minutes in an ultrasonic water bath (Model B1200-R, Branson Ultrasonics Corp., Danbury, CT), and then lyophilized. This treatment, and other treatments designed to produce unaggregated “starting” peptide preparations, have not been found to affect the primary structure of the peptide or its subsequent folding and self-assembly (21, 42-46).

For CD studies, lyophilizates of pretreated peptides were dissolved in 1 volume of water, after which an equal volume of 20 mM phosphate buffer, pH 7.4, containing 0.02% (w/v) sodium azide was added. Samples were sonicated for 1 minute at 22°C , transferred into centrifugal filters (10,000 molecular weight cut off (MWCO), Centricon YM-10, Millipore Corp.), and centrifuged at $16,000 \times g$ using a bench top microcentrifuge (Eppendorf model 5415C, Brinkmann Instruments Inc., Westbury, NY) for 30 min. The filtrate, containing low molecular weight (LMW) A β , was incubated at 22°C without agitation to allow peptide assembly. By definition (47), LMW A β contains monomeric A β in equilibrium with low-order, unstructured oligomers (47-49). The

concentration of A β in the filtrates was determined by quantitative amino acid analysis, as described (50).

For cross-linking experiments of A β 40, LMW A β was isolated using size exclusion chromatography (SEC), as described (41). Briefly, A β was dissolved at a concentration of 2 mg/ml in dimethyl sulfoxide and sonicated for 1 min, after which 170 μl of this solution were injected onto the SEC column. The column was eluted with 10 mM sodium phosphate buffer, pH 7.4, at a flow rate of 0.5 ml/min. Peptides were detected by UV absorbance at 254 nm and fractions of 350 μl volume were collected during elution of the LMW A β peak. The concentrations of Tyr-substituted A β 42 peptides isolated by SEC were lower than those obtained using the centrifugation method (51), therefore the latter method was used to prepare A β 42 peptides for study. Both peptide preparation methods yielded A β solutions that produced CD spectra indicative of predominately disordered secondary structure. Previous studies have shown that LMW A β 42 prepared using filtration or SEC produces similar oligomer distributions in the monomer to octamer region (48). An advantage of the filtration method for preparing A β 42 is that larger oligomers (e.g., dodecamers and octadecamers) are not present (48).

Cross-linking and SDS-PAGE analysis. Peptides were covalently cross-linked using PICUP immediately after preparation (for a review, see (38)). Briefly, 1 μl of 1 mM Tris(2,2'-bipyridyl)dichlororuthenium(II) (Ru(Bpy)) and 1 μl of 20 mM ammonium persulfate in 10 mM sodium phosphate, pH 7.4, were added to 18 μl of a 20–30 μM solution of A β or its analogues immediately after preparation. The mixture was irradiated for 1 s with visible light and the reaction was quenched immediately with 10 μl Tricine sample buffer (Invitrogen, Carlsbad, CA) containing 5% (v/v) β -mercaptoethanol. The cross-linked oligomer mixtures were fractionated by SDS-PAGE using 10–20% Tricine gels (1.0 mm \times 10 well) (Invitrogen), silver stained using a SilverXpress silver staining kit (Invitrogen), and then the band intensities were quantified by densitometry, as described (49). The amounts taken for SDS-

PAGE analyses were adjusted according to the peptide concentration, determined by amino acid analysis, so that equal amounts of protein were loaded in each lane. Gels were dried, scanned, and the intensities and gel mobilities (R_f) of the resulting monomer and oligomers bands quantified by densitometry using the program One-Dscan (Scanalytics, Fairfax, VA). The relative amount of each band in a lane as a percentage of all bands in the same lane was determined according to the formula $I_r^i = (I_i / \sum I_i) \times 100$, where I_i is the intensity of the band i .

Circular dichroism spectroscopy (CD). A β , at a concentration of 30–35 μ M in 10 mM phosphate buffer, pH 7.4, was prepared by filtration and then spectra were acquired daily during incubation of peptides at 22°C without agitation. Samples were prepared for analysis by gently drawing up and then expelling the peptide solution in a 200 μ l pipette tip. After three such cycles, the peptide solution was placed into a 0.1 cm path-length quartz cell (Hellma, Forest Hills, NY). Spectra were acquired using an Aviv Model 62A DS spectropolarimeter (Aviv Associates, Lakewood, NJ). Following measurements, samples were returned to the original sample tubes. All measurements were done at 22°C. Spectra were generally recorded over the wavelength range of 198–260 nm. Three independent experiments were performed with each peptide. Raw data were manipulated by smoothing and subtraction of buffer spectra, according to the manufacturer's instructions.

Spectral deconvolution was performed using the CDPro software package (52), which contains the deconvolution programs SELCON3, CDSSTR, and CONTIN. In this package, reference sets of proteins from different sources are combined to create a large reference set of CD spectra. Depending on the spectrum wavelength range, the number of proteins in the reference set (IBasis) can be as large as 48 (IBasis 7). Deconvolutions were done with each of the three programs. If the data thus obtained were similar, they were averaged to obtain the percentage of each secondary structure element. In some cases, the results obtained from one program were highly

divergent from those of the other two. In this case, averaging was done only with data from the two consistent programs. Deconvolutions were performed on data acquired at the initiation of assembly, when the presence of significant α -helix was observed (by visual inspection of the spectra), and when assembly was complete (spectra remained identical during repeated monitoring). We note that the kinetics of assembly in these studies differ quantitatively, but not qualitatively, from those acquired in previous work (53). Here, the assembly reactions were performed using 20 mM phosphate buffer, pH 7.4. The earlier studies were done in 10 mM Gly-NaOH, pH 7.5. The latter buffer slows the kinetics and facilitates occupation of regions of conformational space containing α -helix.

Thioflavin T (ThT)-binding. A 100 μ l aliquot of each A β sample in 10 mM phosphate buffer, pH 7.4, containing 0.01% (w/v) sodium azide, was mixed with 5 μ l of 100 mM ThT prepared in the same buffer. Immediately after addition of ThT, fluorescence was measured. The measurements were made using a Hitachi F4500 spectrofluorometer (Hitachi Instruments Inc., Rye, NH) with excitation at 450 nm and emission at 480 nm. A rectangular 10 mm quartz microcuvette was used. All fluorescence measurements were carried out at 22°C with a scan rate of 240 nm/min. Slit widths used for excitation and emission were 5 and 10 nm, respectively. Three independent experiments were performed for each peptide.

Electron microscopy (EM). For studies of fibrillar A β , 5 μ l of each sample were spotted on a glow-discharged, carbon-coated Formvar grid (Electron Microscopy Sciences, Fort Washington, PA), incubated for 5 min, washed with distilled water, then stained with 1% (w/v) aqueous uranyl formate. Uranyl formate (Pfaltz & Bauer, Waterbury, CT) solutions were filtered through 0.2 mm sterile syringe filters (Corning) before use. EM analysis was performed using a JEOL 1200 transmission electron microscope. Four independent experiments were carried out for each peptide.

For studies of cross-linked and non-

cross-linked LMW A β peptides, cross-linking reactions were quenched with 1M dithiothreitol (DTT, FisherBiotech, Fair Lawn, NJ) in water instead of 5% (v/v) β -mercaptoethanol in tricine sample buffer (Invitrogen). The same LMW preparation also was cross-linked and quenched immediately with 10 μ l of 5% (v/v) β -mercaptoethanol in tricine sample buffer and then used for SDS-PAGE to verify that the expected oligomer distribution was obtained. Ten μ l of each sample were incubated for ~20 min on the grid. The solution was gently removed using Whatman grade 2 qualitative filter paper and then the grid was incubated with 5 μ l of 2.5% (v/v) glutaraldehyde for 4 min, after which fluid again was removed using filter paper. The peptide then was stained with 5 μ l of 1% (w/v) uranyl acetate (Pfaltz & Bauer) for 3 min. This solution was wicked off and the grid was air-dried. Samples were examined using a JEOL CX100 electron microscope.

Quantitative analysis of oligomer geometry in cross-linked and non-cross-linked LMW A β samples was performed by manual determination of oligomer dimensions by inspection of EM images. A representative sample was obtained with particle number $n=40$. Particle diameter and length statistics were calculated using Mathematica 6.0 (Wolfram Research, Inc., Champaign, IL USA).

Reverse-staining and isolation of individual oligomers. Cross-linked A β oligomers separated by SDS-PAGE were detected by imidazole-zinc staining, essentially as described (54). Briefly, after SDS-PAGE, the gel was rinsed in distilled water for 30 s and then incubated in 0.2 M imidazole (Sigma, St. Louis, MO) solution containing 0.1% (w/v) electrophoresis grade SDS (Fisher Scientific, Pittsburg, PA) for 15 min. The solution then was discarded and the gel was incubated in 0.2 M zinc sulfate in distilled water for ~0.5–1 min, until the gel background became white and the A β oligomers bands were transparent and colorless. Further staining was prevented by rinsing the gel in distilled water. The staining process was monitored by placing the gel in a transparent tray over a piece of black paper. Immediately after staining, the oligomer bands were excised using a scalpel blade (Fisher

Scientific) and placed into 1.5 ml conical microcentrifuge tubes. The gel slices were incubated (2×5 min) in 1 ml of 25 mM ammonium acetate buffer, pH 7.4, containing 100 mM EDTA, during which time the gels become complete colorless. The gel slices then were washed twice (2×5 min) using 25 mM ammonium acetate buffer, pH 7.4, and frozen quickly on dry ice (to make the gels pieces brittle and fragile). The pieces were crushed using a 1.5 ml microcentrifuge tube as a mortar and a geometrically matched pestle (Fisher Scientific). After crushing the gel pieces, the pestle was held over the tube and washed with 25 mM ammonium acetate buffer, pH 7.4, to ensure that all the gel pieces were collected. Additional buffer was added to the tube to make the volume of the resulting suspension twice that of the original gel pieces. The microcentrifuge tube containing the gel suspension then was agitated by moderate vortexing for 10 min using a Multi-Tube Vortexer (VWR International, Bristol, CT). The gel mixture was centrifuged for ~1 min at $14,000 \times g$ and then the supernate was collected and placed in a glass tube. A volume of buffer twice that of the crushed gel was added to the pellet, which then was vortexed for 10 min. After another centrifugation, done as above, the supernate was collected and combined with the first supernate. A volume of 25 mM ammonium acetate, 50% (v/v) acetonitrile, 0.1% (v/v) TFA, equal to that of the pellet then was added to the pellet and the tube was vortexed for 10 min. A third supernate then was obtained by centrifugation and was combined with the first two supernates. Because A β oligomers are hydrophobic, a fourth extraction was done for 10 min using 25 mM ammonium acetate buffer, 25% (v/v) acetonitrile, 25% (v/v) isopropanol, and 0.1% (v/v) TFA. A final extraction was done for 2 min using 80% (v/v) acetonitrile. The pooled supernates were concentrated by centrifugal evaporation (Savant SpeedVac Concentrator, Thermo Scientific, Waltham, MA).

Matrix-Assisted Laser Desorption/Ionization Mass Spectrometry (MALDI-MS). MALDI-MS was performed on a Voyager-DESTR time-of-flight mass spectrometer employing 337 nm

irradiation. The matrices α -cyano-4-hydroxycinnamic acid, sinapinic acid, ferulic acid, 2-mercaptobenzothiazole, norharmane, 2-(4-hydroxyphenylazo)benzoic acid, and 2,5-dihydroxybenzoic acid (DHB) were investigated. The DHB matrix yielded superior spectra and thus was employed for all experiments described here. Mass spectra were acquired in linear and reflector modes. Oligomers were detected most readily in linear mode.

RESULTS

Secondary structure dynamics. To probe amino acid site specific contributions to peptide conformation and assembly, we used circular dichroism spectroscopy (CD) and thioflavin T (ThT) binding to monitor temporal changes in secondary structure. In the CD analyses, A β 40 and its substituted alloforms were predominantly unstructured immediately after preparation, as indicated by prominent negative molar ellipticities at \sim 198 nm (Fig. 2A). Conformational changes in A β 40 were noticeable after \sim 6 d. At day 7, mixed α/β character was indicated qualitatively by double inflections in the 205–225 nm region and quantitatively by spectral deconvolution. Visual inspection suggested that α -helix content was maximal at \sim 8 d. Quantitative analysis of the spectra was done following deconvolution (see Methods). At 0 d, α -helix, β -strand, β -turn and random coil (RC) secondary structure elements were present at levels of \sim 8%, \sim 9%, \sim 6%, and 77%, respectively. In contrast, at 8 d, α -helix, β -strand, β -turn and RC levels were \sim 26%, \sim 24%, \sim 19%, and 33%, respectively. The mixed α/β conformer population at 8 d comprises in part a previously described α -helix-rich intermediate (53). Between days 7–14, an $\alpha/\beta \rightarrow \beta$ transition was observed that produced a classical β -sheet-type spectrum with a negative ellipticity of significant magnitude centered at \sim 215–218 nm. The spectral deconvolution at day 14 showed that the α -helix, β -strand, β -turn, and RC levels were \sim 10%, \sim 66%, \sim 5% and 20%, respectively.

[Phe¹⁰]A β 40, the “scaffold” upon which the Tyr-substituted peptides was built, displayed time-dependent conformational changes

qualitatively similar to that of A β 40, as did the four other Tyr-substituted alloforms. As reported previously in studies of A β 40 assembly (53), absolute convergence of the spectra onto an isodichroic point was not seen, suggesting a multi-state transition process. We do note, however, that some convergence of the spectra to a single point occurred in the [Tyr⁴⁰]A β 40 experiment.

To obtain quantitative insight into the kinetics of the RC $\rightarrow\alpha/\beta\rightarrow\beta$ conformational conversions, we studied the time-dependence of θ_{222} (Supplementary Fig. 1A). The half-time for the development of α -helix structure, and the time at which maximal α -helix structure is observed, are later for [Tyr¹]A β 40 (8.5 and 11 d, respectively) than they are for A β 40 (7 and 8 d, respectively). These two times also are longer than those for [Tyr¹⁰]A β 40 or [Tyr²⁰]A β 40. The half-time for [Tyr³⁰]A β 40 (8 d) is slightly earlier than that of [Tyr¹]A β 40, but the α -helix maximum occurs at least 2 d earlier. [Tyr⁴⁰]A β 40 displays a significantly earlier half-time (7 d) and a slow conformational transition that extends for at least 4 d. Smoothing of these data would suggest that the α -helix maximum for [Tyr⁴⁰]A β 40 occurs at least one day earlier than that in [Tyr¹]A β 40.

Consistent with the CD studies, no ThT binding was observed by any peptides immediately after their preparation (Table 1). However, substantial binding was detected when characteristic β -sheet spectra were seen by CD. Binding levels among the different peptides were equivalent, within experimental error ($FU_{avg}=9475 \pm 598$).

CD analysis revealed that A β 42, [Phe¹⁰]A β 42, and the Tyr-substituted analogues displayed RC $\rightarrow\alpha/\beta\rightarrow\beta$ transitions (Fig. 2B) qualitatively similar to those observed with A β 40, but with accelerated kinetics. Consistent with this acceleration, the observed lifetimes of the α -helix-containing conformers were relatively short (one day instead of 3–5 days in A β 40). The α -rich conformer appeared for all peptides at day 3, except for [Tyr¹]A β 42, in which the α -helix-rich conformer appeared at day 4. The rapidity with which the RC $\rightarrow\alpha/\beta\rightarrow\beta$ transition occurs in the A β 42 peptide family is

indicated by a monotonic decrease in θ_{222} that begins earlier and does not reach the magnitude of those seen in the A β 40 samples (Supplementary Fig. 1B). This increased A β 42 assembly rate is consistent with results of earlier comparative studies of A β 40 and A β 42 peptides linked to familial forms of AD and cerebral amyloid angiopathy (53).

Deconvolution of the A β 42 spectra obtained immediately following preparation of LMW peptides revealed levels of α -helix, β -strand, β -turn, and RC of \sim 4–5% \sim 12–15%, \sim 10–15%, and \sim 65–70%, respectively. At the midpoints of the RC \rightarrow α / β \rightarrow β conformational transitions, levels of α -helix, β -strand, β -turn, and RC were \sim 12–16%, \sim 35%, \sim 20%, and \sim 30%, respectively.

The spectral deconvolution at d8, where all A β 42 spectra were mostly β -sheet (by visual inspection) have suggested that spectra of all A β 42 peptides are consistent with β -sheet (\sim 70%) rich structure. The α -helix and RC content are \sim 5% and \sim 20%, respectively. In contrast to the A β 40 series, an isodichroic point was observed at a wavelength of \sim 210 nm in experiments on the A β 42 peptide series. This point was particularly prominent in A β 42 and [Phe¹⁰]A β 42, but also was present in the four other samples. Interestingly, the most divergent spectra in each of these four samples were obtained at the time of maximal α -helix content, and among these, the [Tyr³⁰]A β 42 was the most divergent. No ThT binding was observed initially, but significant binding was detected when β -sheet-like CD spectra existed (Table 1). With the exception of [Tyr³⁰]A β 42, all the A β 42 peptides bound equivalent amounts of ThT ($FU_{avg}=4641 \pm 1241$). [Tyr³⁰]A β 42 produced \sim 1/2 the ThT fluorescence as did the average A β 42 peptide and the A β 42 average ThT binding was \sim 1/2 that of the average A β 40 peptide.

It should be noted that the reproducibility of studies of A β assembly kinetics depends on careful peptide preparation and manipulation (for a recent review, see (36)). The experiments presented here all were performed using the same peptide lot that was prepared and incubated in precisely the same manner for all samples. Solutions were not

agitated and any study of the reactions was done with minimal perturbation of the tubes. Under these conditions, the kinetics was reproducible within experiments. Absolute changes in kinetics can be observed between experiments, but the rank order of rates of conformational change remain constant among experiments. Thus, peptides that form β -sheet structure fastest in any one experiment always form β -sheet structure fastest. Similarly, the “slowest” peptides always are the slowest. The system variability thus is so small that the trends in rank order of β -sheet formation are always the same.

Morphologic analysis of assemblies. To determine the morphologies of the assemblies present at the completion of the CD and ThT studies, electron microscopy (EM) was done. All twelve peptides formed long, unbranched fibrils with smooth margins (Figs. 3A and 3B). A β 40 produced 8–12 nm diameter fibrils comprising three individual filaments of \sim 3.3 nm diameter twisted into a helical superstructure with a pitch 150–160 nm. [Phe¹⁰]A β 40, [Tyr²⁰]A β 40, and [Tyr⁴⁰]A β 40 fibrils typically were composed of two laterally-associated filaments wound together with a helical pitch of \sim 75–110 nm. [Tyr¹]A β 40 and [Tyr³⁰]A β 40 produced a more structurally diverse population of fibrils that displayed diameters ranging from 6–12 nm and were composed of 2–5 filaments. Some fibrils had no observable twist, whereas others displayed a helical pitch of \sim 100–150 nm.

In contrast to the variation in fibril morphologies observed in the A β 40 samples (Fig. 3A), A β 42 peptides formed fibrils that were morphologically similar (Fig. 3B). Most fibrils were \sim 4–6 nm in diameter and were composed of two filaments. Little discernible substructure was apparent in many fibrils, whereas others appeared with irregular twists or helical twists with pitches of \sim 40–80 nm. The only departure from these shared morphologic features was observed with [Phe¹⁰]A β 42, which produced fibrils with a diameter range, 5–7.5 nm, that overlapped with but was slightly larger than that of the other peptides. The largest fibril comprised three filaments. The approximate two-fold difference in diameter between fibrils formed by A β 40 and A β 42 is consistent with and provides a plausible explanation for the

magnitude of the difference in ThT binding observed between the two peptide families (see above). However, this explanation assumes a linear relationship between ThT binding and fluorescence intensity. It also is possible that variations in average order or self-quenching could account for the observed differences.

Determination of oligomer size distributions. To probe A β oligomerization, LMW fractions of A β and its Tyr-substituted alloforms were isolated and immediately analyzed by PICUP and SDS-PAGE (Fig. 4, Supplementary Table 1). Distinct oligomer size distributions were observed. A β 40 ([Tyr¹⁰]A β 40) produced a mixture comprising predominately monomer (~20%), dimer (~25%), trimer (~25%) and tetramer (~17%), along with small amounts of pentamer (~6%) and hexamer (~3%). The oligomer distribution of [Tyr¹]A β 40 differed from that of A β 40. Presumptive [Tyr¹]A β 40 monomers through trimers electrophoresed slightly faster than wild type monomer, dimers, and trimers. In the gel region corresponding to the native trimer, two bands existed (Fig. 4, closed arrowhead). Above this region, three additional prominent bands were seen. The oligomer distributions of [Tyr²⁰]A β 40, [Tyr³⁰]A β 40, and [Tyr⁴⁰]A β 40 also differed from that of the wild type. A large shift to higher M_r was observed for the presumptive trimer band and higher-order oligomers of [Tyr²⁰]A β 40. The distribution of [Tyr³⁰]A β 40 resembled that of [Tyr¹]A β 40 in that bands 3 and 4 migrated close to each other, like a doublet. In addition, the M_r values for the higher-order oligomers were higher than those of the corresponding A β 40 oligomers and at least one or two higher-order oligomer bands were observed (band 7 and above). Cross-linking of [Tyr⁴⁰]A β 40 produced the greatest number of bands (10). The [Tyr⁴⁰]A β 40 distribution was similar to that of A β 40 in the monomer-trimer region, but a doublet was formed by bands 4 and 5 (see Fig. 4, arrowhead).

All the substitutions caused increases in the number of oligomer bands and the M_r of the highest-order band. These effects were most apparent in the peptides in which substitutions were made at the C-terminus (positions 30 and 40/42). We note also that the migration

differences of dimers and trimers in the substituted peptides relative to A β 40 were greatest in [Tyr²⁰]A β 40 and progressively smaller in [Tyr³⁰]A β 40 and [Tyr⁴⁰]A β 40.

Cross-linking of A β 42 produced a characteristic (48) distribution with nodes at monomer and pentamer. Heptamers were visible clearly. In the [Tyr¹]A β 42 distribution, the predominant oligomer was the tetramer (Fig. 4, closed arrowhead). Interestingly, the oligomer distribution in the [Tyr¹]A β 42 sample was similar to that of the [Tyr¹]A β 40 sample. The M_r values of the bands were lower than those of wild type A β 42 and bands 3 and 4 migrated as a doublet. In addition, a larger number of bands were seen (9 versus 7) and the largest M_r exceeded heptamer. The oligomer distributions of the Tyr²⁰, Tyr³⁰, and Tyr⁴² alloforms showed M_r values of tetramers and higher-order oligomers higher than their A β 42 homologue. In addition, as with A β 40, all the substitutions caused increases in the number of oligomer bands and the M_r of the highest-order band and these effects were most apparent in the peptides in which substitutions were made at the C-terminus (positions 30 and 42).

We note that, at the peptide concentrations used in these experiment, small variations in experimental conditions (peptide and reactant concentrations, temperature, irradiation time, etc.) do not alter significantly the oligomer frequency distributions. These distributions were reproducible among experiments. Importantly, based on careful study of the cross-linking system itself (49) and on results of extensive structure–activity studies (38, 48, 49), the differences observed among samples in the oligomer frequency distribution and M_r values of individual bands are meaningful. The data are not due to random collisional events “captured” by cross-linking.

Determination of oligomer morphology.

To determine whether increased oligomerization propensity, as indicated by expansion of the oligomer distribution range to higher M_r, was reflected in increased oligomer size, EM studies were performed. Among all the peptides studied, A β 40 and [Tyr⁴⁰]A β 40 displayed the largest difference in oligomerization propensity, and thus we determined their morphologies

immediately following isolation by SEC and cross-linking by PICUP (Fig. 5).

Both non-cross-linked and cross-linked A β 40 displayed clusters of relatively amorphous structures with low aspect ratios. The average diameter of the globular structures seen in non-cross-linked A β 40 was 16.0 ± 0.54 nm (white arrow, inset, Fig. 5a) and 93% of these globules had diameters between 12–20 nm (Supplementary Fig. 2A). Aggregates often were observed. Cross-linked A β 40 produced aggregates that were more thread-like in appearance (black arrow, Fig. 5b), but had similar average diameters (15.8 ± 0.61 nm; white arrow, inset, Fig. 5b; and Supplementary Fig. 2B). Short, protofibril-like structures also were observed and these were more frequent in the cross-linked sample. The lengths of these structures varied significantly (~11–111 nm; Supplementary Fig. 2C) but the distribution of average diameter was narrow ($d = 6.2 \pm 0.2$ nm); Supplementary Fig. 2D).

Non-cross-linked [Tyr⁴⁰]A β 40 also produced relatively amorphous globules and thread-like structures (black arrows, Fig. 5c). The average diameter of these particles was 9.7 ± 1 nm (Supplementary Fig. 2E), smaller than that of A β 40. However, the range of lengths of protofibril-like assemblies produced by [Tyr⁴⁰]A β 40 was similar to that of A β 40 (15–100 nm; Supplementary Fig. 2F). The average diameter of the amorphous structures formed in the cross-linked [Tyr⁴⁰]A β 40 sample (white arrows, Fig. 5d), 19.6 ± 0.9 , was approximately twice that of the non-cross-linked peptide and significantly ($p < 0.0001$) larger than that of cross-linked A β 40 (Supplementary Fig. 2G). This increase is consistent with the increased order observed in the SDS-gels of the cross-linked peptides (Fig. 4).

We note, in principle, that a direct correspondence between PICUP and EM may not be observed because the former method uses the denaturing and dissociative characteristics of SDS-PAGE to reveal covalent association among monomers, whereas the latter method requires only adherence of aggregates to a solid support and not their *pre facto* covalent association. Here, however, the data produced by each method are consistent.

Determination of oligomer order. Our analyses of the oligomer size distributions of the Tyr-substituted peptides (Fig. 4) revealed that certain substitutions, e.g., [Tyr¹]A β 40, produced oligomer distributions distinct from those of wild type A β . To determine the oligomer order within the various gel bands, their component peptides were isolated and subjected to MALDI-TOF mass spectrometry. We first determined the mass of all oligomer bands from wild type A β 40 (band numbers are shown with white letters in Fig. 4). Band 1 from A β 40 produced a major peak of 4332 amu with an additional small, broad peak (<5%) of 8574 amu. We assign the 4332 amu peak to the singly protonated A β 40 monomer (theoretical $m/z = 4331$; Fig. 6A). Bands 2, 3, and 4 produced major peaks of 8656, 13010, and 17383 amu, corresponding to dimer, trimer, and tetramer, respectively (Fig. 6A). Masses from the higher-order bands 5 and 6 could not be obtained, likely because the high molecular weight oligomers were present in small quantities or they may not have been desorbed from the MALDI matrices as readily as the smaller oligomers. Mass spectrometric analysis thus confirmed that A β 40 produced a simple oligomer “ladder.”

We next analyzed [Tyr¹]A β 40 (Fig. 6B). Band 1 displayed a mass of 4363 amu, which is the average mass of a singly protonated monomer. In linear mode, band 2 produced two almost equally intense peaks, one at 8741 amu and one at 4380 amu. The ion of 4380 amu is consistent with oxidized [Tyr¹]A β 40 (expected mass of 4379 amu), while 8741 amu is consistent with a dimer in which one monomer is oxidized (expected mass of 8739 amu). A spectral component of mass 4363 amu also was observed, consistent with the presence of unoxidized monomer. Measurements done in reflector mode revealed 1 amu isotope spacings in the 4400 amu region, establishing that doubly-charged ~8800 Da species were not solely responsible for the 4400 amu ions. Band 3 produced major ions of 4388 and 13188 amu, consistent with monomer mass and trimer, respectively. Although the 13188 amu ion is ~100 Da higher in mass than expected for the trimer (13090), it is reasonable to assign it to

trimer as other oligomers clearly could not produce such a mass. Band 4 yielded four significant peaks, the masses of which were 4384, 8767, 13109 and 17475 amu. We assign these to peptide monomer, dimer, trimer and tetramer, respectively. Band 5 displayed five peaks that were consistent in molecular weight with oxidized monomer (4383), oxidized dimer (8757), oxidized trimer (13196), oxidized tetramer (17617), and oxidized pentamer (21943). The data show, as with A β 40, that an oligomer ladder was produced in the SDS-PAGE experiment that comprised neighboring oligomers differing in order by one. Importantly, the combined electrophoretic/spectroscopic analyses reveal that the Tyr¹ substitution significantly alters the M_r of the peptide tetramer and pentamer, but has much less effect on the monomer, dimer, and trimer. As with A β 40 itself, sufficient signal could not be obtained to analyze the presumptive hexamer and heptamer bands of this peptide (Fig. 4, bands 6 and 7).

Despite extensive efforts using a broad range of matrices and solvents, spectra of [Tyr¹]A β 42 oligomers were not obtained. Insolubility did not appear to explain the phenomenon, as the dried analytes dissolved completely in the solvents employed. Rather, the result may be due to: (1) the inability of these oligomers to be incorporated within crystals of the MALDI matrices, perhaps due to their exceptional hydrophobicity; or (2) the disruption of labile covalent bonds or weak non-covalent interactions by the desorption/ionization process.

DISCUSSION

Evidence from *in vitro* and *in vivo* studies suggests that A β oligomers are potent neurotoxins and may be the proximal effectors of the neuronal dysfunction and death occurring in AD (4, 55-57). This strong association of A β oligomers with AD pathogenesis provides a rationale for the performance of studies to elucidate the structural dynamics of oligomerization, in particular how specific residues within A β control the process. To achieve this goal, here we have executed a strategy we term “scanning PICUP” that

employs Tyr in a classical scanning amino acid substitution paradigm.

The use of Tyr, which is highly reactive in the photochemical cross-linking reaction on which PICUP is based, allowed us to simultaneously probe the effects of alteration of specific amino acid side-chains on A β conformational dynamics and to determine how side-chain modifications affected peptide oligomerization. We note that the results thus obtained depend on the local environment of the Tyr residue within the A β monomer (e.g., its solvent accessibility) and on the oligomerization state of this monomer. The data thus reflect the sum of these phenomena. His and Met also may function in the PICUP chemistry, but their reactivity is substantially lower than that of Tyr (58) and thus the data discussed here reflect the activity of the substituted Tyr.

Qualitative analysis of the results of the CD studies of the A β 40 and A β 42 families of peptides comprising wild type and Tyr-substituted homologues showed that each family underwent a RC $\rightarrow\alpha/\beta\rightarrow\beta$ transition, as has been observed in prior studies (39, 53). However, detailed analysis of the results revealed substitution-dependent alterations in folding kinetics and conformer complexity. For each peptide family, the Tyr¹-substituted homologue folded slowest, as assessed by determination of the midpoint of the secondary structure transition from RC $\rightarrow\beta$ -sheet. This type of divergence from the dynamics of the wild type peptide also was observed in PICUP studies of oligomerization and EM studies of fibril formation. The oligomer frequency distribution of the substituted peptide was distinct, with an unusual doublet band apparent in SDS gels of the cross-linked population. It is significant that the Tyr¹ substitution in A β 42 also produced an unusual oligomer distribution, one qualitatively similar to that seen in A β 40, because this datum suggests that the effects of this substitution on the conformational dynamics of the peptide dominate those linked to the presence of Ile⁴¹Ala⁴².

In analyzing SDS-PAGE data such as those discussed above, one generally infers from the M_r of a particular band that it comprises n -order oligomers, where $n = M_r / MW_{monomer}$.

However, this inference is valid only if the electrophoretic behavior of the analyte is ideal. We did not assume ideal behavior and therefore sought to formally determine the M_r of a number of the bands. In doing so, we found that putative [Tyr¹]A β 40 monomers, dimers, and trimers yielded mass spectra consistent with our order calculation. However, the putative tetramers and pentamers did not. Mass spectrometrically-determined molecular weights for bands 4 and 5 were consistent with the masses of tetramers and pentamers, respectively, yet calculation of their M_r values determined electrophoretically suggested they contained trimers and tetramers, respectively. These oligomers thus migrated anomalously. First principles suggest that the anomalously low M_r was due to oligomer compaction. Direct experimental evidence for A β oligomer compaction has been obtained previously in studies of A β 40, A β 42, and homologues thereof (59, 60).

A β assembly involves intramolecular (within monomer) and intermolecular (within oligomers) interactions. Prior experimental and computational studies have revealed that important interaction sites controlling A β fibril formation exist within and adjacent to the central hydrophobic cluster (CHC; Leu¹⁷–Ala²¹) and the C-terminus (48, 61–64). This knowledge has led naturally to the design of potential therapeutic agents targeting these sites, e.g., KLVFF-like peptide inhibitors (for review, see (65)) and inhibitors targeting the A β C-terminus (66, 67). The ability of a single amino acid substitution at the N-terminus (Tyr¹) to alter the oligomer frequency distribution and the assembly kinetics suggests that the N-terminus is not a benign peptide sub-region uninvolved in peptide assembly, as might be inferred from studies of fibril structure (68). It may be argued instead that the contribution of this region in the wild type peptide to the overall assembly energetics is significant but differs in magnitude from the contributions of the CHC and C-terminus. Does this mean that therapeutic attention to this region is unwarranted? We would argue the contrary, namely that if the inhibitory effects of the Tyr¹ substitution can be amplified through selection of an appropriate small molecule inhibitor, that new and potentially efficacious assembly inhibitors may be discovered.

In addition to the CD experiments revealing effects of substitutions on folding kinetics, insights into the complexity of the conformational space of A β were obtained. The lack of a precise isodichroic point in CD spectra from the A β 40 family shows that peptide assembly is not a simple two-state process (69, 70). However, we note that the spectra produced by the Tyr⁴⁰[A β 40] peptide did converge, albeit imprecisely, near a specific point. This convergence does suggest a decrease in the conformational complexity of the system, as is clearly observed in the spectra of A β 42, which display an isodichroic point. The Tyr⁴⁰ substitution in A β 40 thus produces a secondary structure dynamics more akin to that seen in A β 42. Consistent with this conclusion is the fact that the Tyr⁴⁰ substitution in A β 40 substantially extended the highest order of oligomers observed in the PICUP experiments. For A β 42, its conformational dynamics certainly must correlate with the increased hydrophobic surface of the peptide C-terminus, which in turn may affect the stability of a C-terminal hinge (71) or turn (72) and the interactions of the C-terminus with other regions of the peptide monomer, including the CHC. Because A β 40 lacks two C-terminal residues and has not been found to form a turn in this region (72), our data suggest that the Tyr substitution in A β 40 facilitates structural organization of the peptide monomer through interactions of the C-terminus with the CHC. These interactions may stabilize the monomer, restricting its exploration of conformational space and accounting for the quasi-isobestic point in the CD spectra, an observation suggestive of the absence of intermediates in the conformational conversion process. We note, however, that the structural stabilization imparted on the A β 40 peptide by the substitution of Tyr⁴⁰ does not result in an A β 42-like oligomer distribution. An A β 40-like oligomer distribution is maintained.

Our results elucidate the surprisingly complex structural dynamics of the relatively small A β and how peptide segment-specific interactions may control this dynamics. A key determinant of how these interactions occur is the location of hinge or turn regions in the peptide. Evidence exists for turns in the Val²⁴–Lys²⁸ region of A β in fibrils (for a recent review,

see (68)) and in the A β monomer (72, 73), at the C-terminus of A β 42 (71, 72), at Glu²²-Asp²³ in A β 42 (74), and at other sites (62, 75, 76). Such turns bring regions relatively distant in the primary structure into proximity. For example, the turn at Gly²⁵-Asn²⁷ would induce contacts between the CHC and C-terminus, as well as among residues immediately adjacent to the turn itself. In the PICUP experiments reported here, we observed increased frequencies of higher-order oligomers formed by the peptides in which the Tyr was substituted at Ala³⁰, Val⁴⁰, or Ala⁴². A reasonable explanation for these data is the effect of increased hydrophobicity of the substituted Tyr residue relative to the Ala and Val residues replaced. This would increase the stability of conformers in which hydrophobic side-chain packing occurred, as for example among residues forming the C-terminal turn or residues at the interface between the CHC and C-terminal peptide regions. This explanation also provides a mechanistic rationale for the increased oligomerization potential of the N-terminally substituted peptides, in which Tyr replaced Asp. This substitution produces a more hydrophobic N-terminus, the increased solvophobic nature of which would favor intramolecular interactions with the apolar CHC (62). It is interesting in this regard that the N-terminal dipeptide substitution Glu-Val, which also increases the hydrophobicity of this peptide segment, facilitates protofibril formation (77).

In conclusion, one working hypothesis supported by our data is that A β conformational

dynamics and assembly is a *competition* among interacting regions. For example, the ability of the extreme C-terminus of A β 42 to form a stable turn- or hinge-like structure creates a hydrophobic surface that can interact with the CHC to stabilize assembly-competent conformers. Because it lacks Ile⁴¹ and Ala⁴², A β 40 cannot do so, yet the simple substitution of the A β 40 C-terminal Val with Tyr does create a much more "A β 42-like" peptide. The altered C-terminus now "wins" the competition with the N-terminus, an outcome observed *in silico* (62). The effect of Tyr substitution of Asp¹ is mechanistically similar. The substitution increases the stability of N-terminus-CHC interactions, a result consistent with the observed compaction of the Tyr¹-substituted peptides observed in SDS-PAGE. In this case, the N-terminus competes more effectively with the C-terminus. This mechanism suggests that rational targeting of specific A β subregions could be an effective therapeutic strategy. For example, agents could be designed to block C-terminus:CHC interactions by binding to either or both subregions. Alternatively, agents that enhanced this interaction might facilitate fibril formation, which increasing evidence suggests may be protective (78). In fact, recent work has shown that C-terminal fragments of A β , when mixed with the full-length peptide, coaggregate and block the neurotoxic activity of the free peptide (78). Agents that bound to the N-terminus and facilitated its binding to the CHC also could block formation of toxic assemblies.

REFERENCES

1. Hebert, L. E., Scherr, P. A., Bienias, J. L., Bennett, D. A., and Evans, D. A. (2003) *Arch Neurol* **60**, 1119-1122
2. Brookmeyer, R., Johnson, E., Ziegler-Graham, K., and Arrighi, H. M. (2007) *Alzheimer's Dement* **3**, 186-191
3. Kirkitadze, M. D., Bitan, G., and Teplow, D. B. (2002) *J Neurosci Res* **69**, 567-577
4. Klein, W. L., Stine, W. B., Jr., and Teplow, D. B. (2004) *Neurobiol Aging* **25**, 569-580
5. Klyubin, I., Walsh, D. M., Cullen, W. K., Fadeeva, J. V., Anwyl, R., Selkoe, D. J., and Rowan, M. J. (2004) *Eur J Neurosci* **19**, 2839-2846
6. Hardy, J., and Selkoe, D. J. (2002) *Science* **297**, 353-356.
7. Klein, W. L., Krafft, G. A., and Finch, C. E. (2001) *Trends Neurosci* **24**, 219-224
8. Small, D. H. (1998) *Amyloid* **5**, 301-304
9. Haass, C., and Steiner, H. (2001) *Nature Neurosci* **4**, 859-860
10. Shankar, G. M., Bloodgood, B. L., Townsend, M., Walsh, D. M., Selkoe, D. J., and Sabatini, B. L. (2007) *J Neurosci* **27**, 2866-2875
11. McLaurin, J., Kierstead, M. E., Brown, M. E., Hawkes, C. A., Lambermon, M. H.,

- Phinney, A. L., Darabie, A. A., Cousins, J. E., French, J. E., Lan, M. F., Chen, F., Wong, S. S., Mount, H. T., Fraser, P. E., Westaway, D., and St George-Hyslop, P. (2006) *Nature Med* **12**, 801-808
12. Cheng, I. H., Scearce-Levie, K., Legleiter, J., Palop, J. J., Gerstein, H., Bien-Ly, N., Puolivali, J., Lesne, S., Ashe, K. H., Muchowski, P. J., and Mucke, L. (2007) *J Biol Chem* **282**, 23818-23828
13. Walsh, D. M., Klyubin, I., Fadeeva, J. V., Cullen, W. K., Anwyl, R., Wolfe, M. S., Rowan, M. J., and Selkoe, D. J. (2002) *Nature* **416**, 535-539
14. Oda, T., Wals, P., Osterburg, H. H., Johnson, S. A., Pasinetti, G. M., Morgan, T. E., Rozovsky, I., Stine, W. B., Snyder, S. W., Holzman, T. F., Krafft, G. A., and Finch, C. E. (1995) *Exp Neurol* **136**, 22-31
15. Lambert, M. P., Barlow, A. K., Chromy, B. A., Edwards, C., Freed, R., Liosatos, M., Morgan, T. E., Rozovsky, I., Trommer, B., Viola, K. L., Wals, P., Zhang, C., Finch, C. E., Krafft, G. A., and Klein, W. L. (1998) *Proc Natl Acad Sci USA* **95**, 6448-6453
16. Hartley, D. M., Walsh, D. M., Ye, C. P. P., Diehl, T., Vasquez, S., Vassilev, P. M., Teplow, D. B., and Selkoe, D. J. (1999) *J Neurosci* **19**, 8876-8884
17. Chen, Q. S., Kagan, B. L., Hirakura, Y., and Xie, C. W. (2000) *J Neurosci Res* **60**, 65-72
18. Nalbantoglu, J., Tiradosantiago, G., Lahsaini, A., Poirier, J., Goncalves, O., Verge, A., Momoli, F., Welner, S. A., Massicotte, G., Julien, J. P., and Shapiro, M. L. (1997) *Nature* **387**, 500-505
19. Rowan, M. J., Klyubin, I., Cullen, W. K., and Anwyl, R. (2003) *Phil Trans Royal Soc London Series B Biol Sci* **358**, 821-828
20. Westerman, M. A., Cooper-Blacketer, D., Mariash, A., Kotilinek, L., Kawarabayashi, T., Younkin, L. H., Carlson, G. A., Younkin, S. G., and Ashe, K. H. (2002) *J Neurosci* **22**, 1858-1867
21. Dahlgren, K. N., Manelli, A. M., Stine, W. B., Baker, L. K., Krafft, G. A., and LaDu, M. J. (2002) *J Biol Chem* **277**, 32046-32053
22. Wang, H. W., Pasternak, J. F., Kuo, H., Ristic, H., Lambert, M. P., Chromy, B., Viola, K. L., Klein, W. L., Stine, W. B., Krafft, G. A., and Trommer, B. L. (2002) *Brain Res* **924**, 133-140
23. Cleary, J. P., Walsh, D. M., Hofmeister, J. J., Shankar, G. M., Kuskowski, M. A., Selkoe, D. J., and Ashe, K. H. (2005) *Nature Neurosci* **8**, 79-84
24. De Felice, F. G., Vieira, M. N., Saraiva, L. M., Figueroa-Villar, J. D., Garcia-Abreu, J., Liu, R., Chang, L., Klein, W. L., and Ferreira, S. T. (2004) *FASEB J* **18**, 1366-1372
25. Walsh, D. M., Townsend, M., Podlisny, M. B., Shankar, G. M., Fadeeva, J. V., Agnaf, O. E., Hartley, D. M., and Selkoe, D. J. (2005) *J Neurosci* **25**, 2455-2462
26. Head, E., Pop, V., Vasilevko, V., Hill, M., Saing, T., Sarsoza, F., Nistor, M., Christie, L. A., Milton, S., Glabe, C., Barrett, E., and Cribbs, D. (2008) *J Neurosci* **28**, 3555-3566
27. Kelly, B. L., and Ferreira, A. (2006) *J Biol Chem* **22**, 28079-28089
28. White, J. A., Manelli, A. M., Holmberg, K. H., Van Eldik, L. J., and LaDu, M. J. (2005) *Neurobiol Dis* **18**, 459-465
29. Demuro, A., Mina, E., Kaye, R., Milton, S. C., Parker, I., and Glabe, C. G. (2005) *J Biol Chem* **280**, 17294-17300
30. Chong, Y. H., Shin, Y. J., Lee, E. O., Kaye, R., Glabe, C. G., and Tenner, A. J. (2006) *J Biol Chem* **281**, 20315-20325
31. Deshpande, A., Mina, E., Glabe, C., and Busciglio, J. (2006) *J Neurosci* **26**, 6011-6018
32. Lesné, S., Koh, M. T., Kotilinek, L., Kaye, R., Glabe, C. G., Yang, A., Gallagher, M., and Ashe, K. H. (2006) *Nature* **440**, 352-357
33. Townsend, M., Shankar, G. M., Mehta, T., Walsh, D. M., and Selkoe, D. J. (2006) *J Physiol London* **572**, 477-492
34. Iwata, N., Tsubuki, S., Takaki, Y., Watanabe, K., Sekiguchi, M., Hosoki, E., Kawashima-Morishima, M., Lee, H. J., Hama, E., Sekine-Aizawa, Y., and Saido, T. C. (2000) *Nature Med* **6**, 143-150
35. Huang, S.-M., Mouri, A., Kokubo, H., Nakajima, R., Suemoto, T., Higuchi, M., Staufenbiel, M., Noda, Y., Yamaguchi, H., Nabeshima, T., Saido, T. C., and Iwata, N. (2006) *J*

Biol Chem **281**, 17941-17951

36. Teplow, D. B. (2006) *Meth Enzymol* **413**, 20-33
37. Bitan, G. (2006) *Meth Enzymol* **413**, 217-236
38. Bitan, G., and Teplow, D. B. (2004) *Acc Chem Res* **37**, 357-364
39. Maji, S. K., Amsden, J. J., Rothschild, K. J., Condrón, M. M., and Teplow, D. B. (2005) *Biochem* **44**, 13365-13376
40. Fancy, D. A., Denison, C., Kim, K., Xie, Y. Q., Holdeman, T., Amini, F., and Kodadek, T. (2000) *Chem Biol* **7**, 697-708
41. Walsh, D. M., Lomakin, A., Benedek, G. B., Condrón, M. M., and Teplow, D. B. (1997) *J Biol Chem* **272**, 22364-22372
42. Fezoui, Y., Hartley, D. M., Harper, J. D., Khurana, R., Walsh, D. M., Condrón, M. M., Selkoe, D. J., Lansbury, P. T., Fink, A. L., and Teplow, D. B. (2000) *Amyloid Int J Exp Clin Invest* **7**, 166-178
43. Jao, S. C., Ma, K., Talafous, J., Orlando, R., and Zagorski, M. G. (1997) *Amyloid Int J Exp Clin Invest* **4**, 240-252
44. Zagorski, M. G., Yang, J., Shao, H., Ma, K., Zeng, H., and Hong, A. (1999) *Meth Enzymol* **309**, 189-204
45. Stine, W. B., Dahlgren, K. N., Krafft, G. A., and LaDu, M. J. (2003) *J Biol Chem* **278**, 11612-11622
46. LeVine, H., III. (2004) *Anal Biochem* **335**, 81-90
47. Walsh, D. M., Hartley, D. M., Kusumoto, Y., Fezoui, Y., Condrón, M. M., Lomakin, A., Benedek, G. B., Selkoe, D. J., and Teplow, D. B. (1999) *J Biol Chem* **274**, 25945-25952
48. Bitan, G., Kirkitadze, M. D., Lomakin, A., Vollers, S. S., Benedek, G. B., and Teplow, D. B. (2003) *Proc Natl Acad Sci USA* **100**, 330-335
49. Bitan, G., Lomakin, A., and Teplow, D. B. (2001) *J Biol Chem* **276**, 35176-35184
50. Ezra, D., Castillo, U. F., Strobel, G. A., Hess, W. M., Porter, H., Jensen, J. B., Condrón, M. A. M., Teplow, D. B., Sears, J., Maranta, M., Hunter, M., Weber, B., and Yaver, D. (2004) *Microbiology* **150**, 785-793
51. Fradinger, E. A., Maji, S., Lazo, N. D., and Teplow, D. B. (2005) Studying amyloid β -protein assembly. In: Xia, W., and Xu, H. (eds). *Amyloid precursor protein, a practical approach*, CRC Press, Boca Raton, FL
52. Sreerama, N., and Woody, R. W. (2000) *Anal Biochem* **287**, 252-260
53. Kirkitadze, M. D., Condrón, M. M., and Teplow, D. B. (2001) *J Mol Biol* **312**, 1103-1119
54. Castellanos-Serra, L., Proenza, W., Huerta, V., Moritz, R. L., and Simpson, R. J. (1999) *Electrophoresis* **20**, 732-737
55. Walsh, D. M., and Selkoe, D. J. (2004) *Protein Pept Lett* **11**, 213-228
56. Haass, C., and Selkoe, D. J. (2007) *Nature Rev Mol Cell Biol* **8**, 101-112
57. Walsh, D. M., and Selkoe, D. J. (2007) *J Neurochem* **101**, 1172-1184
58. Kotzyba-Hibert, F., Kapfer, I., and Goeldner, M. (1995) *Angew. Chem. Int. Ed. Engl.* **34**, 1296-1312
59. Bernstein, S. L., Wytttenbach, T., Baumketner, A., Shea, J. E., Bitan, G., Teplow, D. B., and Bowers, M. T. (2005) *J Am Chem Soc* **127**, 2075-2084
60. Baumketner, A., Bernstein, S. L., Wytttenbach, T., Bitan, G., Teplow, D. B., Bowers, M. T., and Shea, J.-E. (2006) *Protein Sci* **15**, 420-428
61. Morimoto, A., Irie, K., Murakami, K., Masuda, Y., Ohigashi, H., Nagao, M., Fukuda, H., Shimizu, T., and Shirasawa, T. (2004) *J Biol Chem* **279**, 52781-52788
62. Urbanc, B., Cruz, L., Yun, S., Buldyrev, S. V., Bitan, G., Teplow, D. B., and Stanley, H. E. (2004) *Proc Natl Acad Sci USA* **101**, 17345-17350
63. Hilbich, C., Kisters-Woike, B., Reed, J., Masters, C. L., and Beyreuther, K. (1992) *J Mol Biol* **228**, 460-473
64. Wood, S. J., Wetzell, R., Martin, J. D., and Hurler, M. R. (1995) *Biochem* **34**, 724-730
65. Mason, J. M., Kokkoni, N., Stott, K., and Doig, A. J. (2003) *Curr Opin Struct Biol* **13**, 526-532
66. Hetenyi, C., Szabo, Z., Klement, E., Datki, Z., Kortvelyesi, T., Zarandi, M., and Penke,

- B. (2002) *Biochem Biophys Res Comm* **292**, 931-936
67. Szegedi, V., Fulop, L., Farkas, T., Rozsa, E., Robotka, H., Kis, Z., Penke, Z., Horvath, S., Molnar, Z., Datki, Z., Soos, K., Toldi, J., Budai, D., Zarandi, M., and Penke, B. (2005) *Neurobiol Dis* **18**, 499-508
68. Tycko, R. (2006) *Q Rev Biophys* **39**, 1-55
69. Chellgren, B. W., Miller, A. F., and Creamer, T. P. (2006) *J Mol Biol* **361**, 362-371
70. Fandrich, M., Forge, V., Buder, K., Kittler, M., Dobson, C. M., and Diekmann, S. (2003) *Proc Natl Acad Sci USA* **100**, 15463-15468
71. Lansbury, P. T., Jr., Costa, P. R., Griffiths, J. M., Simon, E. J., Auger, M., Halverson, K. J., Kocisko, D. A., Hendsch, Z. S., Ashburn, T. T., Spencer, R. G., and et al. (1995) *Nature Struct Biol* **2**, 990-998
72. Lazo, N. D., Grant, M. A., Condrón, M. C., Rigby, A. C., and Teplow, D. B. (2005) *Protein Sci* **14**, 1581-1596
73. Grant, M. A., Lazo, N. D., Lomakin, A., Condrón, M. M., Arai, H., Yamin, G., Rigby, A. C., and Teplow, D. B. (2007) *Proc Natl Acad Sci USA* **104**, 16522-16527
74. Murakami, K., Irie, K., Ohigashi, H., Hara, H., Nagao, M., Shimizu, T., and Shirasawa, T. (2005) *J Am Chem Soc* **127**, 15168-15174
75. Williams, A. D., Portelius, E., Kheterpal, I., Guo, J. T., Cook, K. D., Xu, Y., and Wetzel, R. (2004) *J Mol Biol* **335**, 833-842
76. Hilbich, C., Kisters-Woike, B., Reed, J., Masters, C. L., and Beyreuther, K. (1991) *J Mol Biol* **218**, 149-163
77. Qahwash, I., Weiland, K. L., Lu, Y. F., Sarver, R. W., Kletzien, R. F., and Yan, R. Q. (2003) *J Biol Chem* **278**, 23187-23195
78. Fradinger, E. A., Monien, B. H., Urbanc, B., Lomakin, A., Tan, M., Li, H., Spring, S. M., Condrón, M. M., Cruz, L., Xie, C. W., Benedek, G. B., and Bitan, G. (2008) *Proc Natl Acad Sci USA* **105**, 14175-14180

FOOTNOTES

[†]We thank Drs. Erica Fradinger, Noel Lazo, Marina D. Kirkitadze, Hilal Lashuel, and Alexander Sobol for valuable suggestions and critical comments. This work was supported by grants AG018921, AG027818, and RR020004 from the National Institutes of Health and by a Zenith Award from the Alzheimer's Association. The UCLA Mass Spectrometry and Proteomics Technology Center was established and equipped by a generous gift from the W.M. Keck Foundation.

The abbreviations used are: A β , amyloid β -protein; AD, Alzheimer's disease; A β 40, A β (1-40); A β 42, A β (1-42); CD, circular dichroism; CHC, central hydrophobic cluster; EM, electron microscopy; FU, fluorescence units; LMW, low molecular weight; MALDI-MS, Matrix-Assisted Laser Desorption/Ionization Mass Spectrometry; PICUP, Photo-Induced Cross-linking of Unmodified Proteins; RC, random coil¹; RP-HPLC, reverse phase-high performance liquid chromatography.

¹-We use the term "random coil" (RC) to refer to an irregular conformational state characterized by a relative lack of well-defined structural elements such as α -helices, β -sheets, or β -turns. We do not suggest that this state is truly random in nature.

FIGURE LEGENDS

Fig 1. Primary structure of A β peptides. The sequences of wild type A β 40 and A β 42 are presented, under which are the sequences of the substituted peptides. Hyphens indicate identical amino acid residues. In peptides in which the Tyr probe was placed at positions other than the native position 10, a Phe group was

substituted at position 10. For simplicity, these A β homologues are specified only by the position of the Tyr, i.e., [Tyr[#]]A β 40/42. The complete peptide specification would include the positions of both the Tyr and Phe residues, e.g., [Tyr[#], Phe¹⁰]A β 40/42.

Fig. 2. Secondary structure dynamics. (A) A β 40 and homologues were incubated in 10 mM phosphate buffer, pH 7.4, at 22°C. CD spectra were acquired daily for 14 days. The day on which a spectrum was acquired is indicated by “d#.” The spectra shown are the average of six scans each with an averaging time of five seconds. (B) A β 42 and homologues were analyzed in the same manner. Results for both sets of peptides are representative of those obtained in each of four independent experiments.

Fig. 3. Morphology of A β assemblies. Following peptide assembly, transmission electron microscopy (TEM) was performed on negatively stained samples of: (A) A β 40 and homologues; or (B) A β 42 and homologues. The numerous, small (<5 nm), translucent background structures visible to various degrees in the panels are not proteinaceous but rather are artifacts of the staining procedure. Protein structures of these sizes are not observed in experiments in which fibril formation is allowed to proceed to completion. Scale bars are 100 nm. Insets in panel A are higher magnification images of the respective fields. The insets are 133 nm square. Arrows delimit helical pitches discussed in the text.

Fig. 4. Oligomer size distributions. (A) A β 40 and homologues were cross-linked using PICUP and then oligomer frequency distributions were determined by SDS-PAGE followed by silver staining. Molecular masses of protein standards are shown on the left. The gels are representative of each of 3 independent experiments. (B) A β 42 and homologues analyzed as in (A). The arrowheads indicate regions in which band migration differed from that of the corresponding wild type peptide (see text). White numbers specify band numbers.

Fig. 5. Morphologic analysis of cross-linked peptides. The morphologies of: (a, c) un-cross-linked (–PICUP) and (b, d) cross-linked (+PICUP) wild type and Tyr¹-substituted A β 40 peptides, respectively, was determined by EM of negatively stained preparations. Scale bars are 100 nm. The images are representative of those in each of at least three independent experiments. Arrows identify structures discussed in the text.

Fig. 6. MALDI-TOF MS analysis of isolated oligomers. Bands produced by (A) A β 40 and (B) [Tyr¹]A β 40 following PICUP and SDS-PAGE were identified by negative staining of the gels, after which the protein components were eluted and analyzed mass spectrometrically (see Methods). Normalized ion intensities are presented on the ordinates and mass-to-charge (m/z) ratios are presented on the abscissas. Band numbers and the locations of specific oligomers within the spectra are indicated. Insets show the actual gel lanes from which the bands were isolated.

Table 1. ThT binding^a

<i>Peptide</i>	I_0	I_t
[Phe ¹⁰]A β 40	40 \pm 11	9897 \pm 698
[Tyr ¹]A β 40	36 \pm 12	10199 \pm 501
A β 40	18 \pm 6	9014 \pm 416
[Tyr ²⁰]A β 40	21 \pm 8	9936 \pm 406
[Tyr ³⁰]A β 40	32 \pm 9	8890 \pm 355
[Tyr ⁴⁰]A β 40	42 \pm 16	8912 \pm 358
[Phe ¹⁰]A β 42	37 \pm 8	5607 \pm 644
[Tyr ¹]A β 42	46 \pm 10	4651 \pm 696
A β 42	42 \pm 12	5609 \pm 502
[Tyr ²⁰]A β 42	43 \pm 5	4950 \pm 749
[Tyr ³⁰]A β 42	39 \pm 7	2250 \pm 825
[Tyr ⁴²]A β 42	51 \pm 14	4780 \pm 612

^a Peptide samples were incubated at 22°C at a concentration of ~30 μ M in 10 mM phosphate, pH 7.4. ThT fluorescence intensity (I) was determined, as described in Methods, immediately after peptide preparation (I_0) or after assembly was complete (I_t =14 d for A β 40 or 8d for A β 42), as judged by CD. I is in units of FU \pm S.D, where the units are arbitrary.

Fig. 1



Fig. 2A

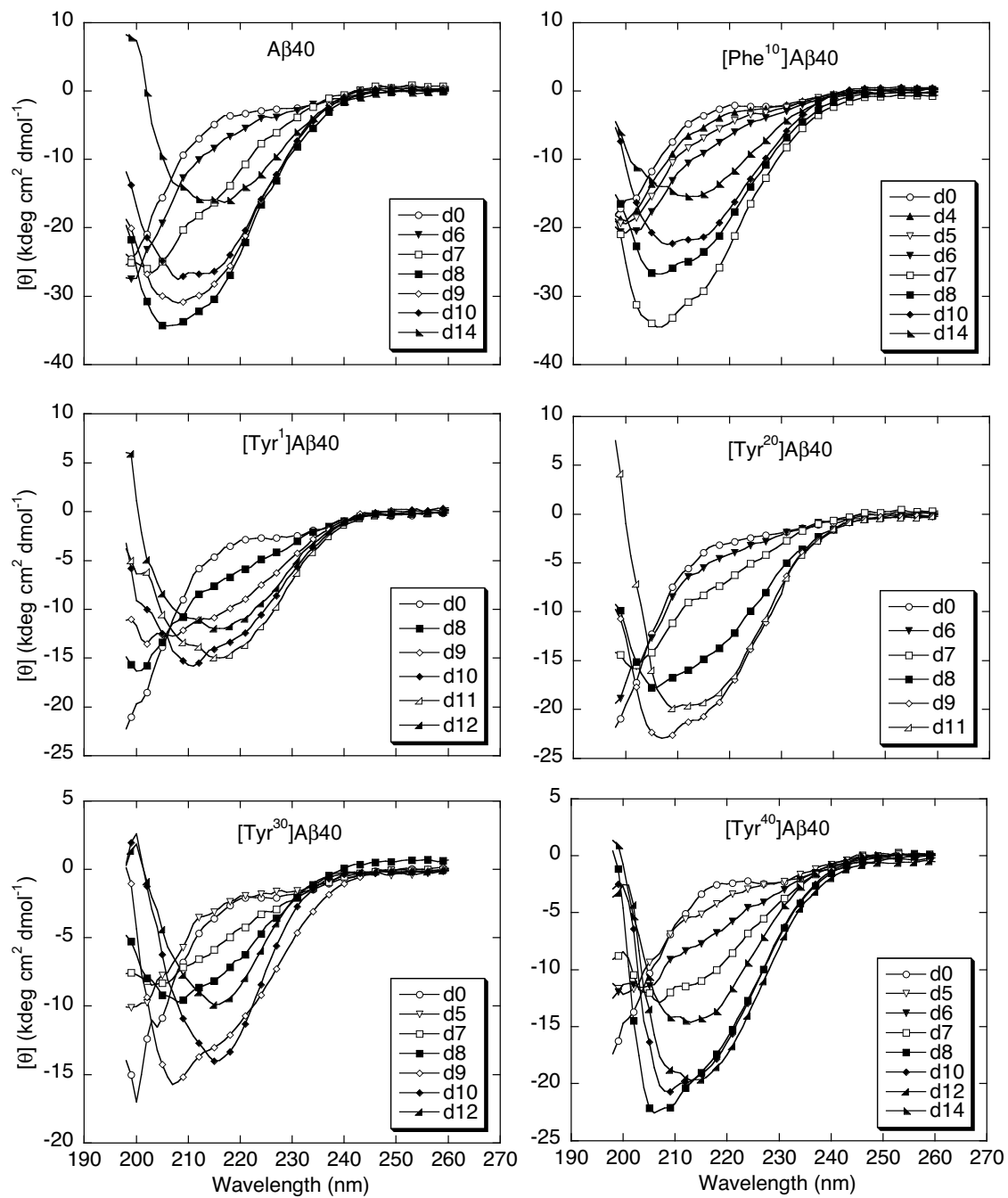


Fig. 2B

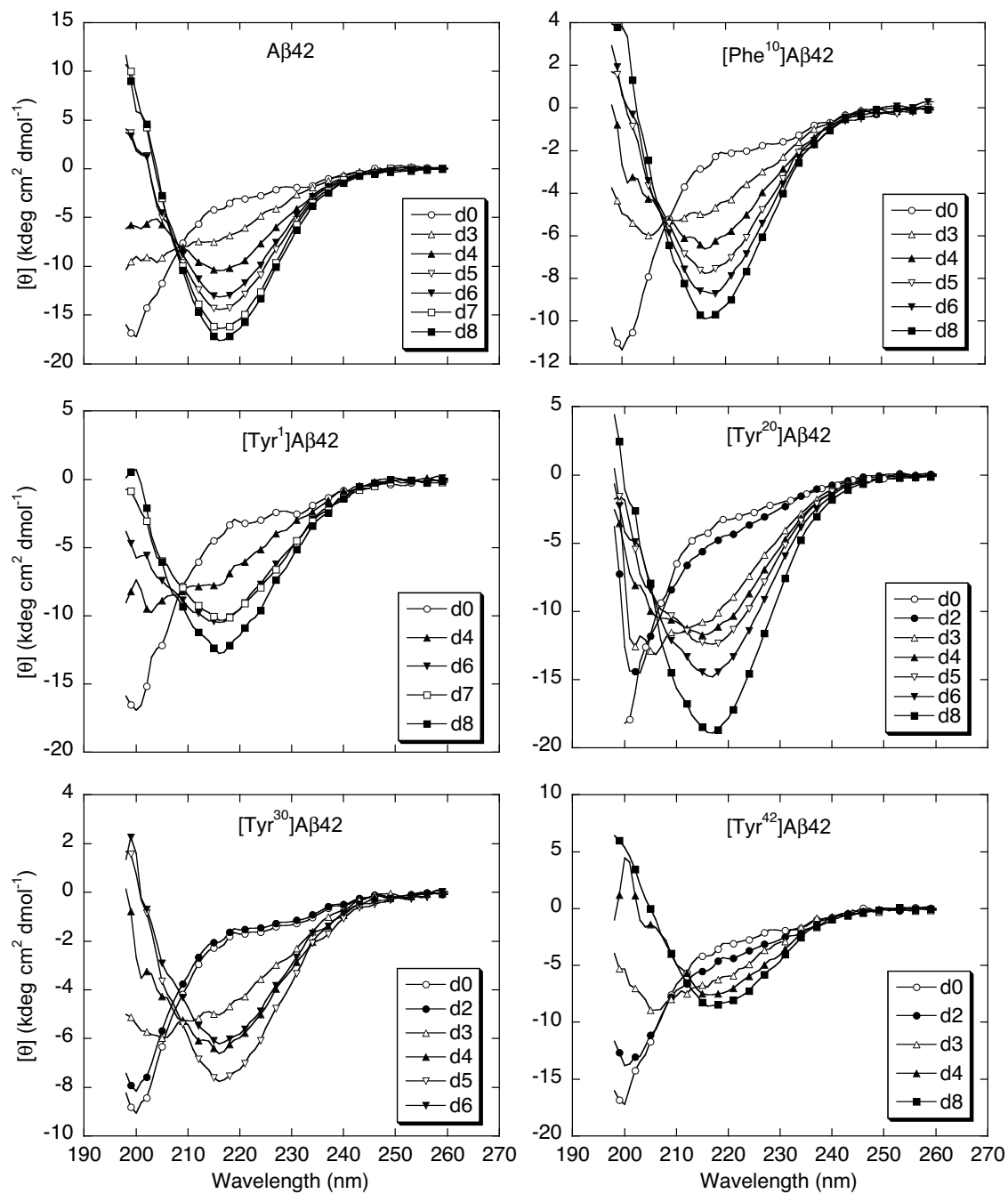


Fig. 3A

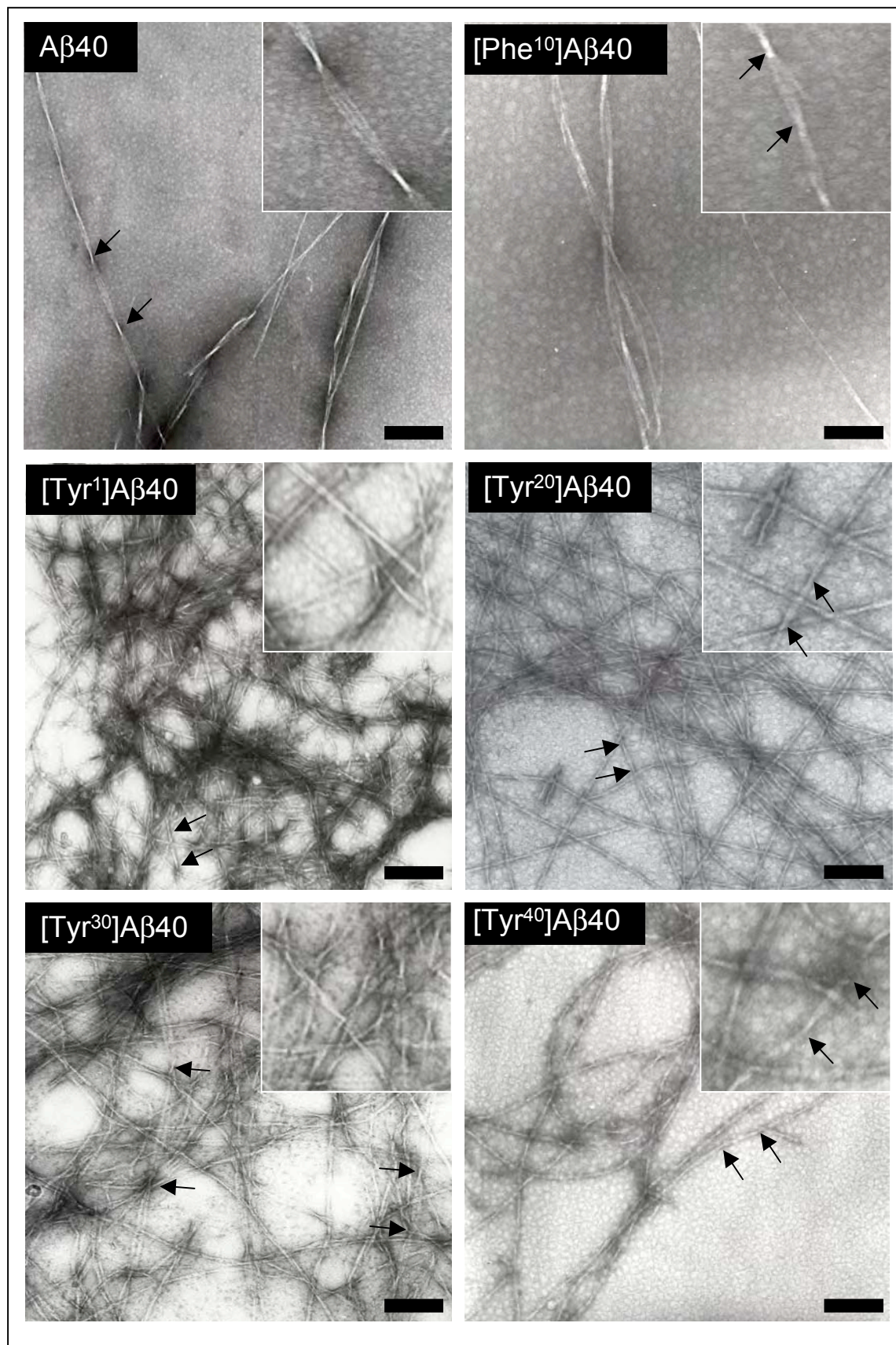


Fig. 3B

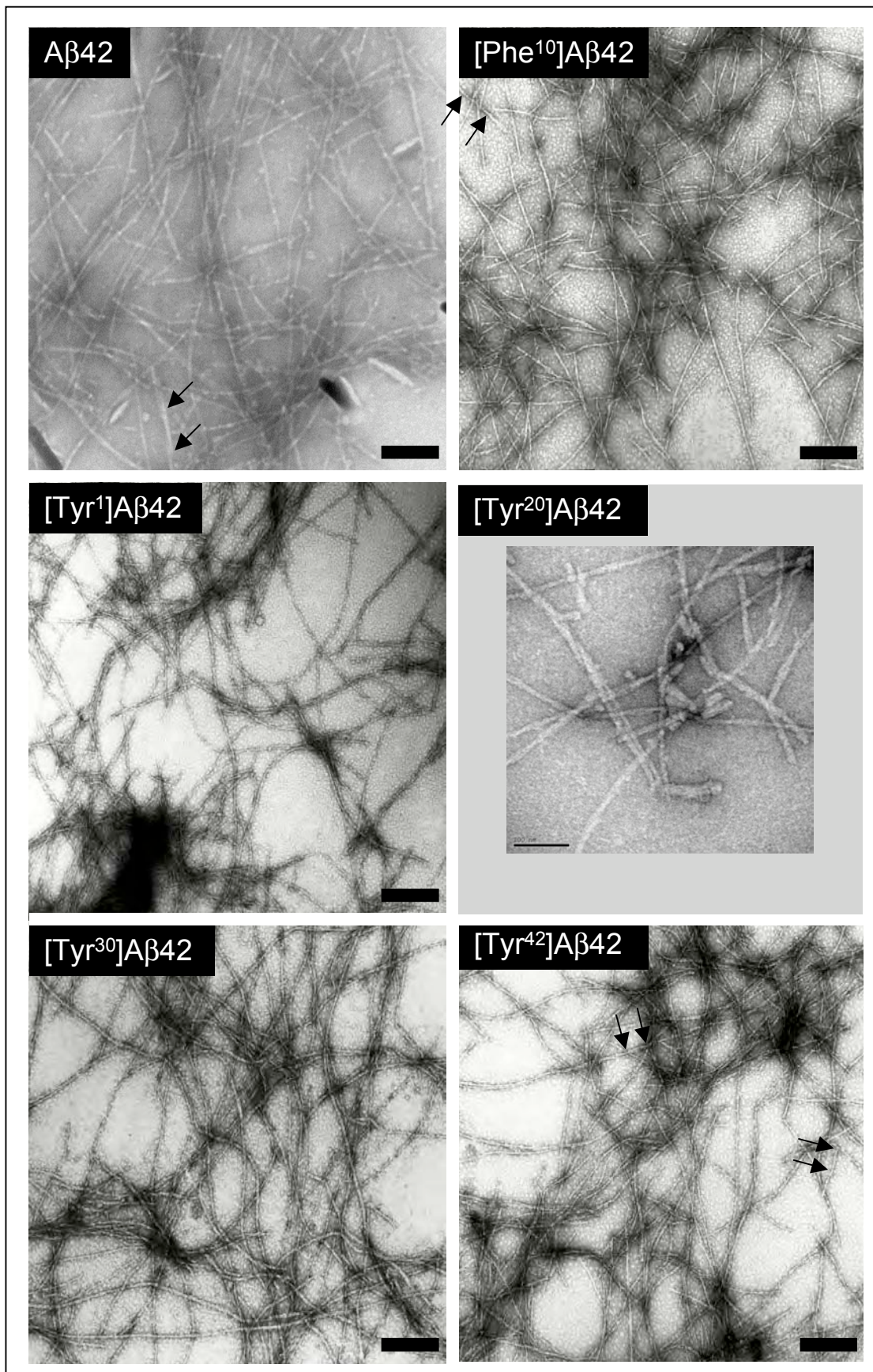


Fig. 4

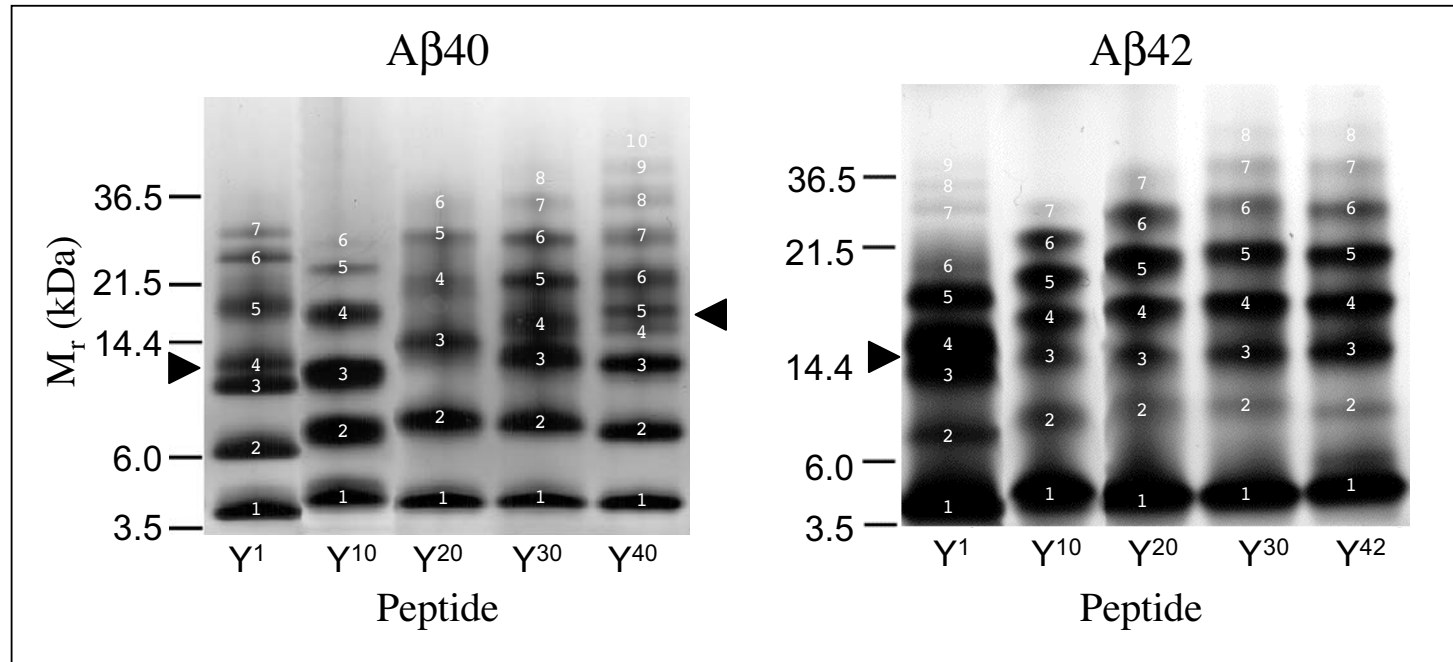


Fig. 5

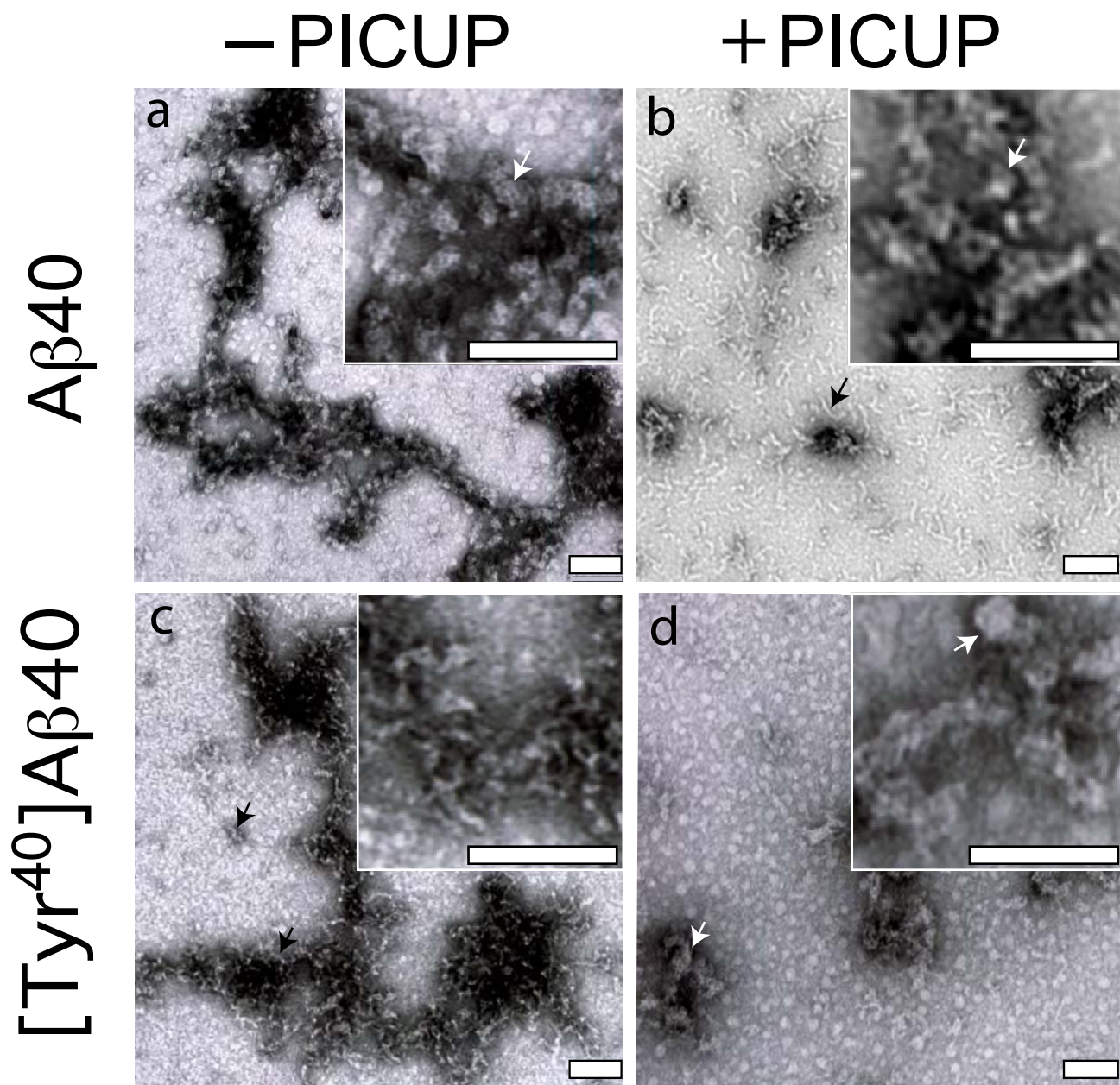
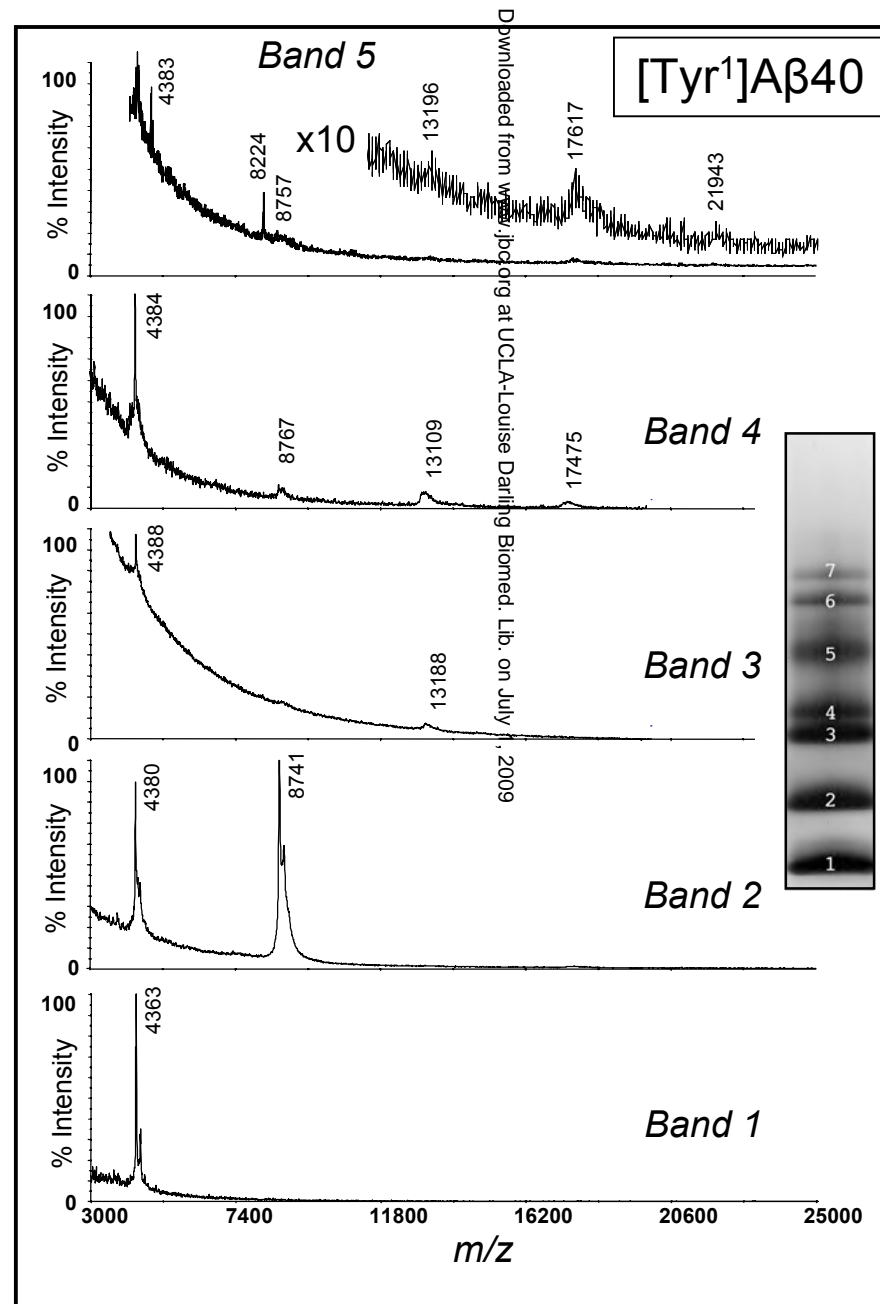
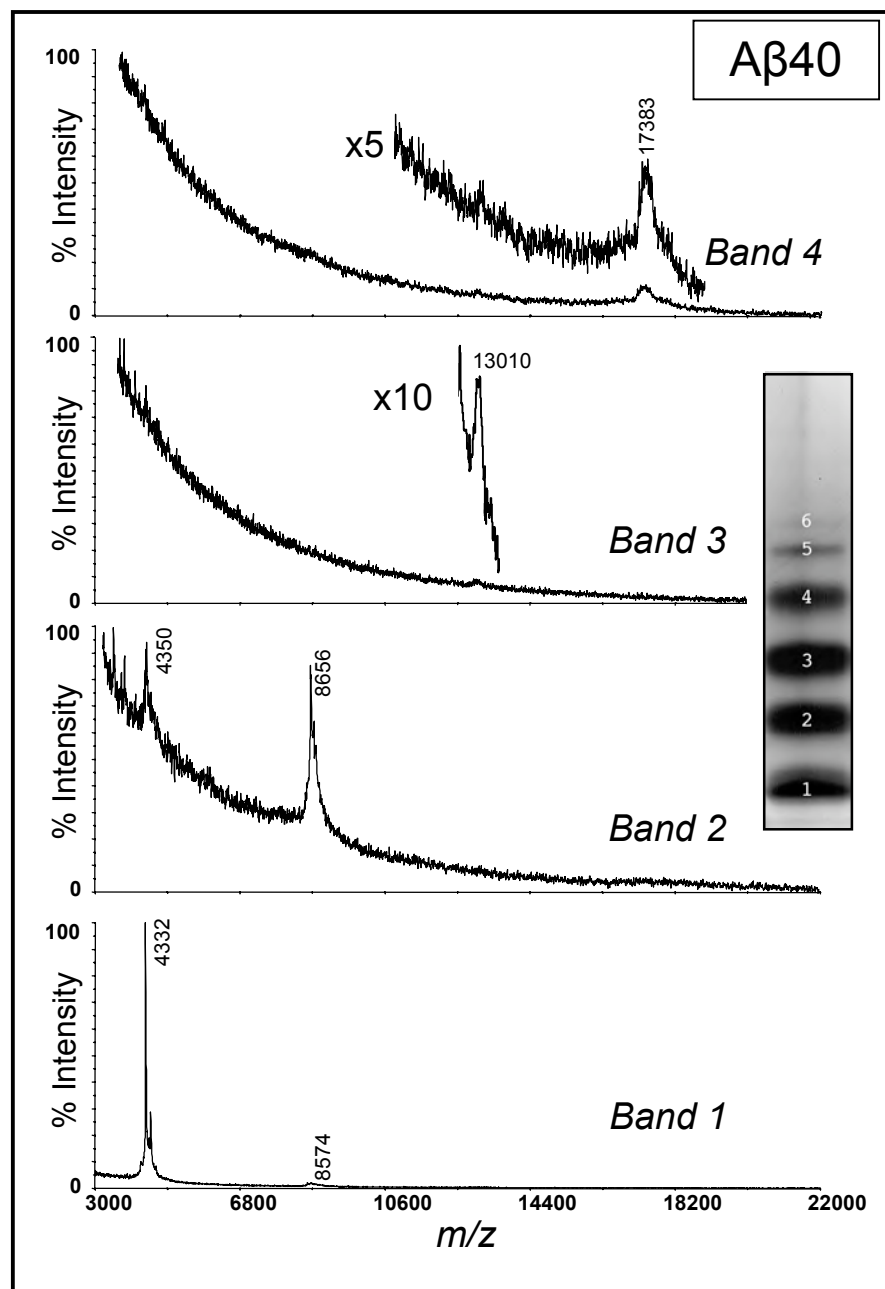


Fig. 6



Downloaded from www.jbc.org at UCLA-Louise Darling Biomed. Lib. on July 1, 2009

SUPPLEMENTARY MATERIALS

AMINO ACID POSITION-SPECIFIC CONTRIBUTIONS TO AMYLOID β -PROTEIN OLIGOMERIZATION[†]

Samir K. Maji^{1,6}, Rachel R. Ogorzalek Loo^{2,3}, Mohammed Inayathullah¹, Sean M. Spring¹, Sabrina S. Vollers^{1,7}, Margaret M. Condrón¹, Gal Bitan^{1,3,4}, Joseph A. Loo^{2,3,5}, and David B. Teplow^{1,3,4,*}

From ¹Department of Neurology and ²Department of Biological Chemistry, David Geffen School of Medicine; ³Molecular Biology Institute; ⁴Brain Research Institute; and ⁵Department of Chemistry and Biochemistry, University of California, Los Angeles, California 90095

Running title: Control of A β oligomerization

⁶Current address: Laboratory of Physical Chemistry, ETH Zurich, CH-8093 Zurich, Switzerland

⁷Current address: Department of Biochemistry and Molecular Pharmacology, University of Massachusetts Medical School, Worcester, MA 01655

*Address correspondence to: David B. Teplow, Ph.D., 635 Charles E. Young Drive South (Room 445), Los Angeles, CA 90095-7334; E-Mail: dteplow@ucla.edu

Table S1. Electrophoretic migration of A β oligomers^a

Band^b	[Y¹]Aβ₄₀	Aβ₄₀	[Y²⁰]Aβ₄₀	[Y³⁰]Aβ₄₀	[Y⁴⁰]Aβ₄₀	[Y¹]Aβ₄₂	Aβ₄₂	[Y²⁰]Aβ₄₂	[Y³⁰]Aβ₄₂	[Y⁴²]Aβ₄₂
1	0.874	0.845	0.847	0.848	0.852	0.851	0.841	0.850	0.854	0.835
2	0.746	0.703	0.678	0.688	0.701	0.719	0.680	0.654	0.654	0.667
3	0.609	0.578	0.517	0.556	0.563	0.538	0.545	0.540	0.539	0.530
4	0.563	0.460	0.395	0.483	0.486	0.509	0.458	0.43	0.426	0.424
5	0.444	0.367	0.305	0.395	0.451	0.413	0.364	0.322	0.316	0.317
6	0.344	0.318	0.249	0.308	0.390	0.355	0.280	0.224	0.209	0.217
7	0.294	–	–	0.230	0.304	0.216	0.216	0.149	0.126	0.123
8	–	–	–	–	0.223	0.164	–	–	–	–
9	–	–	–	–	0.159	0.123	–	–	–	–

^a R_f values for the bands shown in Fig. 5 are listed. ^bBand numbers are referenced to the monomer band, which is #1, and increase in magnitude with decreasing R_f values.

FIGURE LEGENDS

Fig. S1. Kinetic analysis of CD data. To obtain quantitative insight into the kinetics of the $RC \rightarrow \alpha/\beta \rightarrow \beta$ conformational conversions monitored by CD, we plot the time-dependence of θ_{222} . For systems that display significant population of α -helix states, θ_{222} is a useful estimator of α -helix content. For systems that display rapid α -helix \rightarrow β -sheet conversions, θ_{222} can be used as an estimator of overall conversion rate, but not α -helix *per se*, because θ_{222} is correlated with $\theta_{215-218}$, a measure of β -sheet content. (A) A β 40. The half-time for the development of α -helix structure is defined as the time at which θ_{222} has a value equal to half the difference between its maximum and minimum values. The time at which maximal α -helix structure occurs is defined by the point of inflection at the θ_{222} minimum. (B) A β 42. Conversions in this system occur at a rate approximately twice that of A β 40. The kinetic analysis thus provides information on the sum of the rates of conversion from $RC \rightarrow \alpha$ and $\alpha \rightarrow \beta$. No minimum is observed in the A β 42 system. This is because CD is especially sensitive to α -helix, which produces a greater absolute value of θ than is seen with β -sheet. For the A β 40 peptides, the α -helix intermediates we have reported before (see Kirkitadze *et al.* (2001) *J. Mol. Biol.* 312:1103–1119) can accumulate because of the rate differences between its formation (causing θ_{222} of greater magnitude) and its conversion to fibrils (causing θ_{218} of greater magnitude, but less than that of θ_{222}). In contrast, for A β 42, the maximum α -helix content is low (versus A β 40) and the $\alpha/\beta \rightarrow \beta$ transition occurs rapidly, so that the increasing magnitude of the θ_{218} compensates for the loss of the θ_{222} signal and a minimum is not observed. θ just keeps going down (more negative).

Fig. S2. Frequency distributions of particles examined by EM. Oligomer dimensions were determined by inspection of EM images with lens and graticule. A representative sample was obtained with particle number $n=40$. Distributions are shown for: (A), diameters of globular forms of un-cross-linked A β 40; (B), diameters of globular forms of cross-linked A β 40; (C), lengths of protofibrillar forms of A β 40; (D), diameters of protofibrillar forms of A β 40; (E), diameters of globular forms of [Tyr⁴⁰]A β 40; (F), lengths of protofibrillar forms of [Tyr⁴⁰]A β 40; and (G), diameters of globular forms of cross-linked [Tyr⁴⁰]A β 40.

Fig. S1A

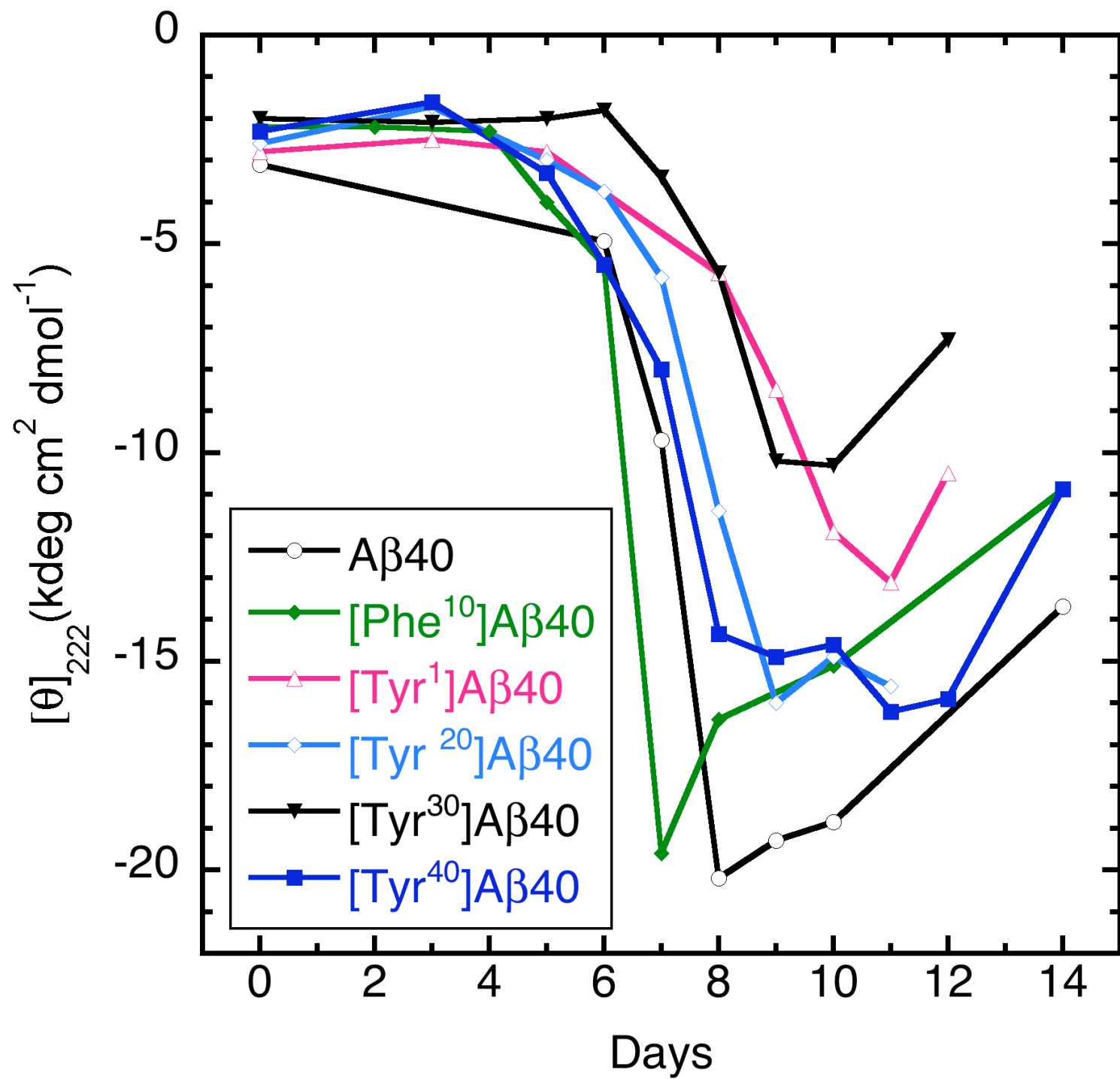


Fig. S1B

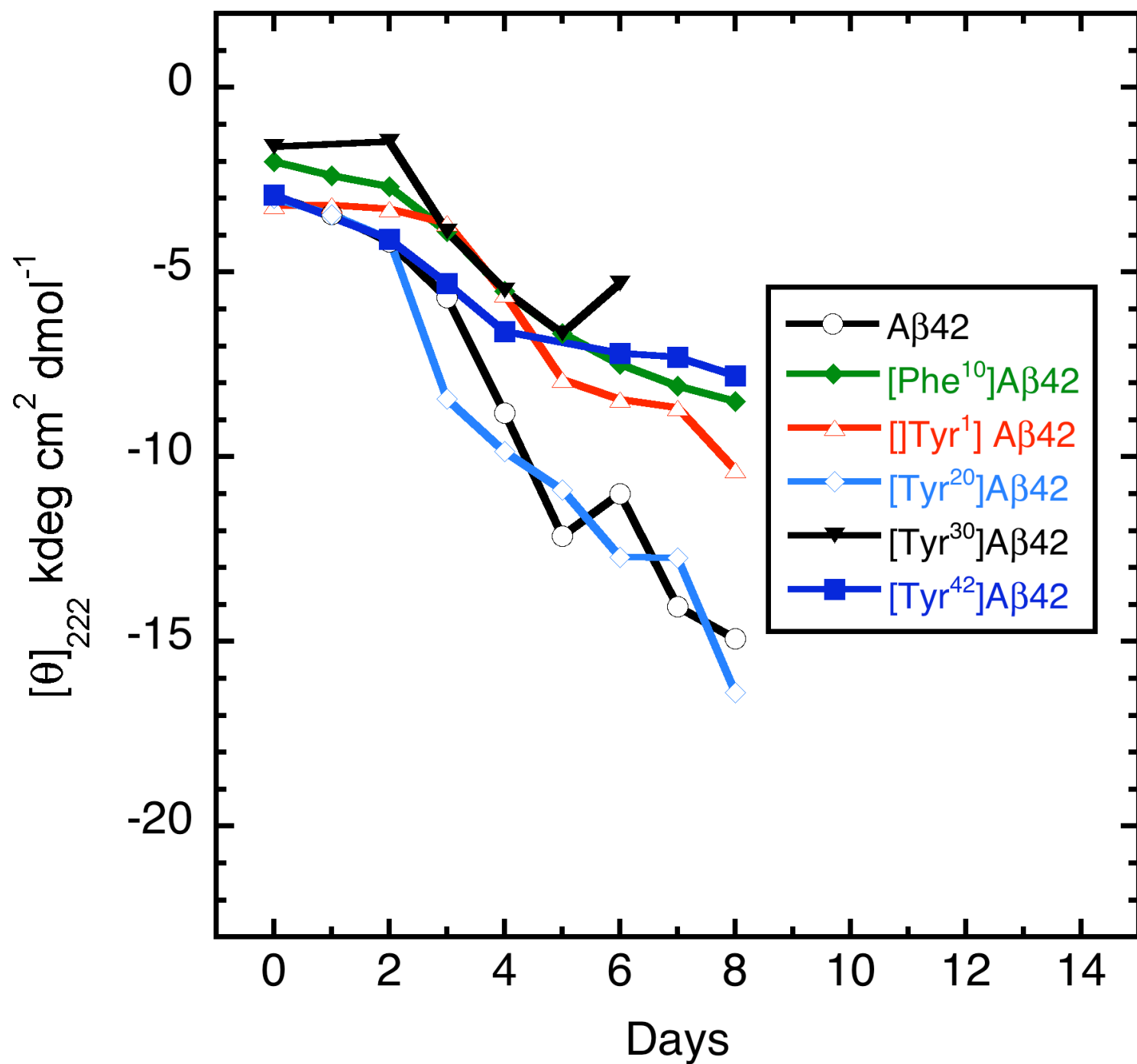


Fig. S2

